Journal of Environmental Management 244 (2019) 208–227

Contents lists available at ScienceDirect

Journal of Environmental Management

journal homepage: www.elsevier.com/locate/jenvman

Research article

Ecosystem service value assessment of a natural reserve region for strengthening protection and conservation

Srikanta Sannigrahi[a,*], Suman Chakraborti[b], Pawan Kumar Joshi[c], Saskia Keesstra[d,e], Somnath Sen[a], Saikat Kumar Paul[a], Urs Kreuter[f], Paul C. Sutton[g], Shouvik Jha[h], Kinh Bac Dang[i,j]

[a] Department of Architecture and Regional Planning, Indian Institute of Technology Kharagpur, 721302, India
[b] Center for the Study of Regional Development (CSRD), Jawaharlal Nehru University, New Delhi, 110067, India
[c] School of Environmental Sciences (SES), Jawaharlal Nehru University, New Delhi, 110067, India
[d] Soil, Water and Land-use Team, Wageningen University and Research, Droevendaalsesteeg3, 6708PB, Wageningen, Netherlands
[e] Civil, Surveying and Environmental Engineering, The University of Newcastle, Callaghan, 2308, Australia
[f] Department of Ecosystem Science and Management, Texas A&M University, College Station, TX, 77843-2120, USA
[g] Department of Geography and the Environment, University of Denver, 2050 East Iliff, Avenue, Denver, CO, 80208-0710, USA
[h] Indian Centre for Climate and Societal Impacts Research (ICCSIR), Kachchh, Gujarat, 370465, India
[i] Institute for Natural Resource Conservation, Department of Ecosystem Management, Christian Albrechts University Kiel, Olshausenstr. 40, 24098, Kiel, Germany
[j] Faculty of Geography, VNU University of Science, 334 Nguyen Trai, Thanh Xuan, Hanoi, Viet Nam

ARTICLE INFO

Keywords:
Ecosystem services
Ecosystem service values
Spatiotemporal
Land use
Remote sensing
Sundarbans
Mangrove ecosystems

ABSTRACT

Ecosystem Services (ESs) refer to the direct and indirect contributions of ecosystems to human well-being and subsistence. Ecosystem valuation is an approach to assign monetary values to an ecosystem and its key ecosystem goods and services, generally referred to as Ecosystem Service Value (ESV). We have measured spatiotemporal ESV of 17 key ESs of Sundarbans Biosphere Reserve (SBR) in India using temporal remote sensing (RS) data (for years 1973, 1988, 2003, 2013, and 2018). These mangrove ecosystems are crucial for providing valuable supporting, regulatory, provisioning, and cultural ecosystem services. We have adopted supervised machine learning algorithms for classifying the region into different ecosystem units. Among the used machine learning models, Support Vector Machine (SVM) and Random Forest (RF) algorithms performed the most accurate and produced the best classification estimates with maximum kappa and an overall accuracy value. The maximum ESV (derived from both adjusted and non-adjusted units, million US$ year^{-1}) is produced by mangrove forest, followed by the coastal estuary, cropland, inland wetland, mixed vegetation, and finally urban land. Out of all the ESs, the waste treatment (WT) service is the dominant ecosystem service of SBR. Additionally, the mangrove ecosystem was found to be the most sensitive to land use and land cover changes. The synergy and trade-offs between the ESs are closely associated with the spatial extent. Therefore, accurate estimates of ES valuation and mapping can be a robust tool for assessing the effects of poor decision making and overexploitation of natural resources on ESs.

1. Introduction

Ecosystem Services (ESs) refer to the bundle of goods and services which are indispensable for human well-being and subsistence (Costanza et al., 1997, 2014; Braat and De Groot, 2012; MEA (Millennium Ecosystem Assessment), 2005), whereas, ecosystem function (EF) refers to the processes and components that occur within an ecosystem (Braat and De Groot, 2012). The 'Ecosystem Service Values (ESVs)' is an approach to quantify and assign economic value to ecosystem goods and services and its functions. Due to growing demand and overexploitation of natural resources, the structure and function of an ecosystem are severely affected at local to global scale (Liu et al., 2017; TEEB, 2010; Song and Deng, 2017). The coastal wetland including mangrove, the freshwater swamp forest ecosystems, are providing valuable regulatory (storm protection, preventing coastal erosion, nutrient cycling, waste treatment, habitat provision), supporting

* Corresponding author.
E-mail addresses: srikanta.arp.iitkgp@gmail.com (S. Sannigrahi), suman87_ssf@jnu.ac.in (S. Chakraborti), pkjoshi27@hotmail.com (P.K. Joshi), saskia.keesstra@wur.nl (S. Keesstra), snsen@arp.iitkgp.ac.in (S. Sen), skpaul@arp.iitkgp.ac.in (S.K. Paul), urs@tamu.edu (U. Kreuter), paul.sutton@du.edu (P.C. Sutton), jhashouvik@gmail.com (S. Jha), dbac@ecology.uni-kiel.de (K.B. Dang).

https://doi.org/10.1016/j.jenvman.2019.04.095
Received 13 November 2018; Received in revised form 20 April 2019; Accepted 22 April 2019
Available online 22 May 2019
0301-4797/

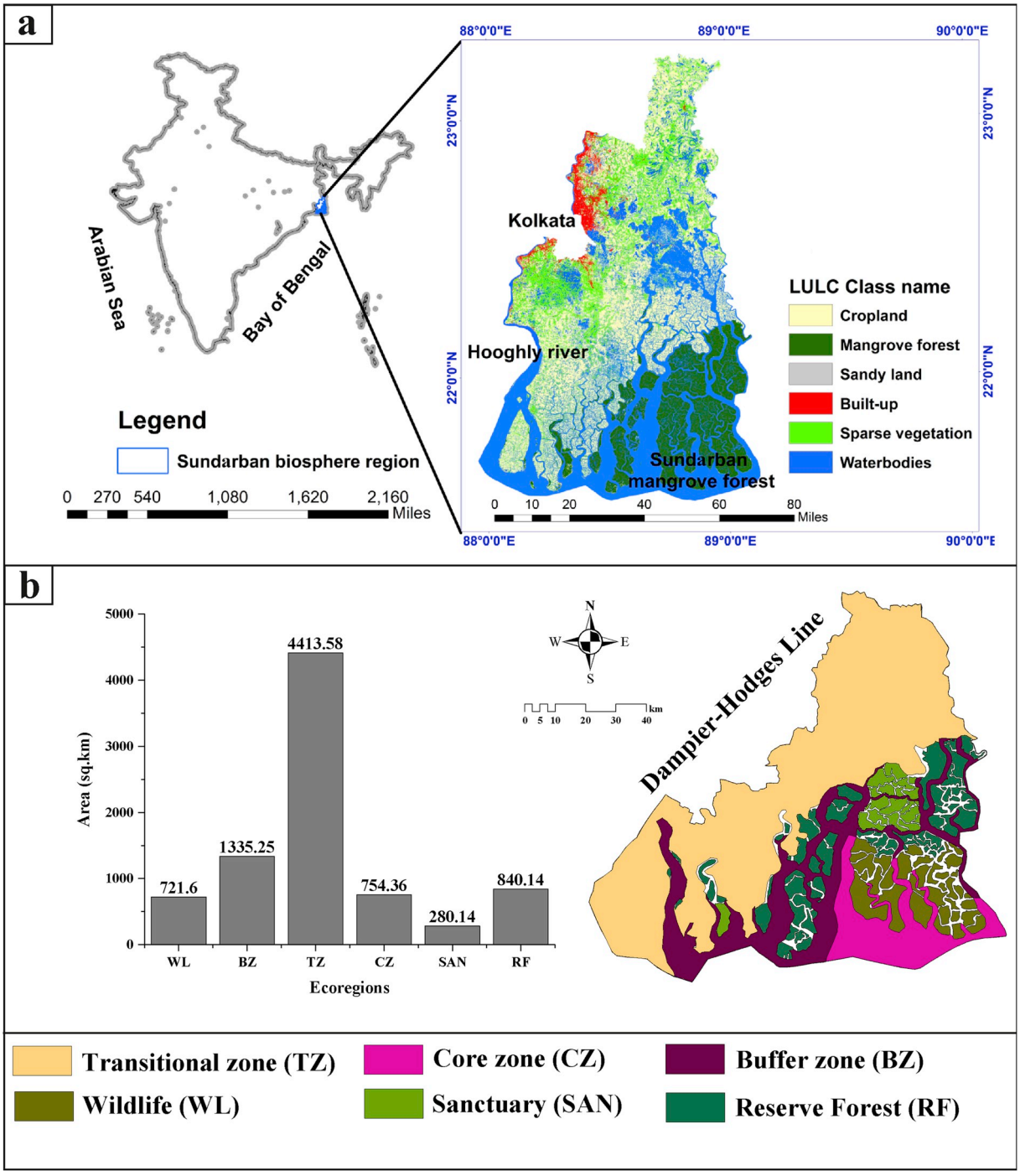

Fig. 1. (a) Location of the study area and **(b)** descriptions of the major eco-regions of Sundarban biosphere region.

(biomass production), provisioning (fish, crab, honey, timber production) and cultural services (De Groot et al., 2002; Ren et al., 2016). Thus most of the coastal communities are directly and indirectly rely on these services for their livelihood and well-being. There are numerous studies on ecosystem services. However, it is challenging to accurately measure the biophysical economic values of ecosystem services due to over/underestimation and double counting. In general, the natural reserve region provides highly valuable ESs across the ecosystems (Liu et al., 2017; Wang et al., 2014; Xu et al., 2017a,b; Yu and Han, 2016). The rate of degradation of natural reserve ecosystems is gradually increasing with time. This is due to persistent demand for various ESs, mainly provisioning services, for human well-being. However, the overexploitation of natural resources especially in the coastal natural reserve region disrupts the native ecosystem structure and its services (Viña and Liu, 2017; Liu et al., 2017; Bruel et al., 2010; Curran, 2004) and in most of the cases, protection, and conservation interests are limited to preservation of engendered species only. Apart from the benefits of long-term species conservation and management, ecosystems also have the potentiality to produce multiple ecosystem goods, services, and functions (Viña and Liu, 2017).

The recent advancement in geospatial science and its broad applications in ES studies, including spatially explicit value transfer and ESs modeling are found to be useful for its cost and time benefits. However, in reality, the quantification of ESV of natural ecosystem is difficult, as a limited valuation market exists to capture the costs of many indirect services (carbon sequestration, gas regulation, climate regulation, etc.)

that makes these services invisible to its economic benefits (Curtis, 2004; Vo et al., 2012). Several approaches have evolved and incorporated in estimating use and non-use service values that explicitly includes market price and benefit transfer approaches (Costanza et al., 1997, 2014; De Groot et al., 2012; Troy and Wilson, 2006; Wilson and Hoehn, 2006). Whereas, other valuation methods consist of contingent valuation (CV), avoided cost (AC), reclamation cost (RC), production approach (P), hedonic pricing (HP), conjoint analysis (CA), travel cost (TC), replacement cost (RC) approaches among other (Vo et al., 2012; De Groot et al., 2012), and spatial explicit biophysical modeling approach (Costanza et al., 2008; Nelson et al., 2009; Boumans et al., 2002).

In this study, we have tried to quantify and map valuable ESs of Sundarbans Biosphere Regions (SBR), a natural reserve region, known as a unique ecosystem. The Sundarbans mangrove forest is the largest mangrove patch in the world (Giri et al., 2007). This ecosystem is well known for its environmental connotation, and it is significant for storm/flood protection, biodiversity maintenance, habitat provision, erosion control, nutrient recycling, and waste treatment services. Additionally, millions of people depend on this ecosystem for their daily livelihoods and subsistence. In spite of having a great significance in protecting the natural and human resources and providing a substantial amount of ecosystem goods and services, little efforts have been made to effectively quantify and assess the economic importance of this vibrant ecosystem. The objectives of this study were to (1) classify the region into several ecosystem types using ten supervised machine learning algorithms; (2) estimated the economic values of multiple key ESs of a natural reserve region using an adjusted equivalent value coefficient; (3) evaluate the effects of landscape changes on ESs and functions using both global and adjusted local coefficients; (4) identify the most sensitive and vulnerable ecosystems using the coefficient of sensitivity, coefficient of elasticity, coordination degree, and ES sensitivity index. There are several studies on the economic importance of ecosystem services, but this study contributes and improves the existing literature by having machine learning methods with spatially explicit techniques.

2. Materials and methods

2.1. Study area

Sundarbans biosphere region is located in the confluence of the rivers Ganga, the Brahmaputra, and Meghna with an aerial extent of 10,000 km^2 (India's share 40%, and Bangladesh's share 60%), of which 4264 km^2 is under intertidal zone (Mandal et al., 2009). The mangrove cover is subdivided into two main subsystems: (1) forest and (2) aquatic (1781 km^2). The region was declared as a zone of ecological importance and came under part of the Man and Biosphere Programme of UNESCO on 29th March 1989. The reserve region is subdivided into several protected areas namely the Sundarban National Park, Sundarban Tiger Reserve, wildlife sanctuaries (i.e., Sajnekhali, Haliday Island and the Lothian Island). The landward limit of this region is determined by the Dampier-Hodges line (Fig. 1). Nandy & Kushwaha (2011) classified this biosphere region into four major sub-regions, i.e., the core zone (1700 km^2), a buffer zone (2400 km^2), restoration zone (230 km^2), and the development zone (5300 km^2). The landscape of the region is mainly composed of tidal creeks, tidal/mudflats, salt marsh waterways, high and low mangroves. The Sundarbans region along with the offshore and inshore zones of the Bay of Bengal (BoB) is very dynamic due to constant interaction of two contrasting environments of land and sea. This region is known for its high ecological and biological productivity due to a continuous supply of nutrient-rich elements and organic matter from mangrove litter (Datta et al., 2017; Rakshit et al., 2015; Mandal et al., 2013; Mandal et al., 2012). The forest of Sundarbans can be classified as littoral swamp forest, including freshwater and mangrove swamps mainly determined by the distribution of salinity. The climate of the region is a tropical humid with the three significant seasonal monsoonal periods, southern monsoon (June–September), post-monsoon (October–January), and pre-monsoon (February–May) (Nandy and Kushwaha, 2010).

2.2. Land use land cover (LULC) classification

Multi-source remote sensing data products were used to map and quantify the distribution of different ecosystems. In the ES valuation research, defining ecoregions is the most important for its success in deriving ESV. For this purpose, Landsat Multi-Spectral Scanner (MSS) for 1973, Thematic Mapper (TM) for 1988, 2003, and Operational Land Imager (OLI) for 2013 and 2018 with path 138, and rows 044 and 045 were used to classify the regions into seven major ecoregions. Except for the data of 1973, the radiometrically and geometrically calibrated Landsat data products were retrieved from EarthExplorer (https://earthexplorer.usgs.gov/) and thoroughly been used for subsequent analyses. However, in order to remove the seasonal differences and maintain the consistency in classification, satellite data collected in December/January month with less than 10% cloud coverage were used.

The data were classified into six major eco-regions, i.e. cropland, mixed/natural vegetation, mangrove, waterbody, sandy coast, and urban using supervised machine learning algorithms [i.e., Artificial Neural Network (ANN), Decision Tree (DT), Bayes, Gradient Boosted Tree (GBT), Linear Discriminant Analysis (LDA), K Means Nearest Neighbour (KNN), Maximum Likelihood Classification (MLC), Support Vector Machine (SVM Linear and Radial Basis Function – RBF), Random Forest (RF)]. The usefulness of machine learning algorithm is instrumental for large scale mapping and in the data-sparse environment that makes it a more successful in recent literature (Liu et al., 2017; Maxwell et al., 2018; Zhu et al., 2017; Sannigrahi et al., 2017, 2018; Janalipour and Mohammadzadeh, 2017). However, no such single method is exemplary for obtaining multiple ecosystems. This study has chosen various classification techniques, and among them, the best model is used for the input of ES calculation in each respective year. In the classification process, the waterbody category was further divided into two separate units, i.e., coastal estuary and inland wetland for valuation of ESs. An average of 50–60 training sample features was extracted for each ecoregion to perform the classification. The ENVI 5.3 software system was used for the SVM and maximum likelihood classification, IDRISI TerrSet software was used for the KNN and LDA algorithms, the EnMAP-Box suite for ENVI 5.3 was used to perform the RF algorithm, and QGIS Orfeo ToolBox (OTB) was used for ANN, BAYES, DT, GBT, and SVM models. Afterward, a 4×4 majority filter was applied to remove isolated pixels from the thematic layers. The conversion of land from one unit to another was measured through a uniform spatial harmonization approach, designed for multiple reference periods. Additionally, a transpose matrix was developed to measure the LULC transformation among the ecosystem types. The spatiotemporal changes in different LULC categories were measured as follows:

$$\Delta LULC_i = \frac{LULC_{End} - LULC_{Start}}{LULC_{Start}} \times 100 \quad (1)$$

$$LUCI = \frac{LULC_{End} - LULC_{Start}}{LULC_{Start}} \times \frac{1}{t} \times 100 \quad (2)$$

where, $\Delta LULC_i$ is the change in land use land cover during the reference period$_i$, $LULC_{End}$ and $LULC_{Start}$ is the area of a particular land use unit at the ending and starting time, $LUCI$ is change intensity of LULC category$_i$, t is the reference period for which estimation was made.

2.2.1. Accuracy assessment of thematic layers

The reliability and accuracy of the classified images were verified through several accuracy assessments test, including the User's

Accuracy (UA) denotes user's perception in classifying an earthed object, Producer's Accuracy (PA) is referring to the proportion of the area of each ecosystem types or earth objects in the ground that are correctly mapped, Overall Accuracy (OA) denotes the percentage of sample units that are correctly associated with the reference or classified thematic layer, and Kappa coefficient is based on the concept of 'random allocation agreement'. However, the uses of kappa in classification accuracy assessment have severely criticized by many studies (Pontius and Millones, 2011; Stehman and Wickham, 2011) and recommend to not go for kappa while assessing the accuracy of LULC results (Olofsson et al., 2013). Following the Olofsson et al. (2013, 2014) schemes of classification and accuracy assessment, in this study, we have performed the entire LULC classification analysis by several steps (1) classified the region into six major eco-regions using 10 machine learning algorithms; (2) evaluated the thematic accuracy of the classified products through several standard accuracy statistics including UA, PA, OA, and kappa coefficient; (3) estimated the total area proportion, class area estimates using visual sample units for assessing the precision of land use classification and identification of mapping errors; and (4) quantified the variance of estimates, standard errors of area estimates, and confidence intervals for both 95% and 99% level for the error-free area approximation.

For evaluating the accuracy and precision of the classification outputs, we used 50–60 visual sample units for different reference years (Congalton, 1991). The validation sample units were extracted from the Google Earth (GE) imagery and historical land use maps of the Sundarbans for multiple assessment years (Yang et al., 2017). For all reference years, 85–95% overall accuracy was obtained for all machine learning algorithms, and among them, the best-classified output was chosen for the ES valuation and mapping.

For computing the estimated area proportion of class k, two different proportion parameters, i.e., map classification parameter $p_{k\cdot}$ and reference classification parameter $p_{\cdot k}$ were used. Due to classification error and uncertainties, the map classification parameter produces biased estimation than that of reference classification parameter. The 'good practice' guidelines by Olofsson et al. (2014) proposed that reference classification parameter producing relatively higher quality estimates and low standard error compared to map classification parameter and area estimation of land classes should be based on the reference parameter.

After that, for class k, the direct estimate of the proportion of area can be calculated as

$$\hat{p}_{\cdot k} = \sum_{i=1}^{q} \hat{p}_{ik\cdot} \tag{3}$$

where $\hat{p}_{\cdot k}$ is the proportion of area derived from the reference classification parameter, q is error matrix, $\hat{p}_{ik\cdot}$ is the area proportion of category k. However, for the simple random, systematic, or stratified random sampling design with map classification strata, stratified estimates of the proportion of area can be calculated as

$$\hat{p}_{\cdot k} = \sum_{i=1}^{q} W_i \times \frac{n_{ik}}{n_i} \tag{4}$$

where W_i is the area proportion of map class i, $n$is the sample counts of k. The standard error for stratified estimates of proportion was measured as

$$S\left(\hat{p}_{\cdot k}\right) = \sqrt{\sum_i W_i^2 \frac{\frac{n_{ik}}{n_{i\cdot}}\left(1 - \left(\frac{n_{ik}}{n_{i\cdot}}\right)\right)}{n_{i\cdot} - 1}} = \sqrt{\sum_i \frac{W_i \hat{p}_{ik} - \hat{p}^2_{ik}}{n_{i\cdot} - 1}} \tag{5}$$

where, $S(\hat{p}_{\cdot k})$ is a standard error of area estimates, n_{ik} is sample count at cell (i, k), W_i is area proportion of class i. In addition to this, the area of class k is the function of $\hat{A}_k = A \times S(\hat{p}_k)$ where A is the area. Furthermore, the standard error of the estimated area at 99% and 95% confidence interval is measured as

$$S\left(\hat{A}_k\right) = A_k \times S(\hat{p}_{\cdot k}). \tag{6}$$

$$CI95\% = \hat{A}_k \pm 1.96 \times S\left(\hat{A}_k\right)$$

$$CI99\% = \hat{A}_k \pm 2.58 \times S\left(\hat{A}_k\right) \tag{7}$$

where, $CI95\%$ and $CI99\%$ are confidence intervals at 95% and 99% level, $S\left(\hat{A}_k\right)$ is a standard error of the estimated area (Stehman and Wickham, 2011; Olofsson et al., 2013, 2014; Wagner and Stehman, 2015; Khatami et al., 2017).

2.2.2. Similarity and dissimilarity assessment of the classification outputs

As the LULC maps were prepared using different classification algorithms; therefore, it is necessary to capture the inter-model variability of the classification output. In that case, the kappa and other conventional accuracy measures fail to capture such spatial variability. Therefore, different similarity and dissimilarity matrices including Spearman Dissimilarity (SD), Gower Coefficient (GC), Cosine Similarity (CS), Percent of Agreement (PA), Bray-Curtis Dissimilarity (BCD), Chi-Square Distance (CSD), Kendall Dissimilarity (KD), Pearson Dissimilarity (PD), and Percent of Disagreement (PED) were used, to select the model more robust in classification assessment. The (dis)similarity measures between two components reflect the dependency and independence between two elements (X, Y) in a sequence, where, the X and Y represent the estimates from two objects in a sequence. Moreover, a binary similarity estimate, Jaccard Coefficient for evaluating the spatial (dis)association of the model estimates combining all reference years was performed. Total 26,133 sample points were used to perform the similarity and dissimilarity of the model outputs. Map classification information derived from a series of machine learning models was extracted through a grid scale for the whole study region. Additionally, all the classified ecoregions were transformed into a discrete unit to perform the mentioned test.

2.3. Estimation of ecosystem service values

2.3.1. Determining equivalent weight coefficient

Developing a robust and identical equivalent weight coefficient is the precondition for estimation of per unit ESVs of an ecosystem (Costanza et al., 1997, 2014; Xie et al., 2003, 2008, 2017). We choose 17 main ESs, i.e. gas regulation (GR), climate regulation (CR), disturbance regulation (DR), water regulation (WR), water supply (WS), erosional control (EC), soil formation (SF), nutrient cycling (NC), waste treatment (WT), pollination (POL), biological control (BC), habitat (HA), food production (FP), raw materials (RM), genetic resources (GEN), recreation (REC), and cultural (CUL) services from the study of Costanza et al., (2017). The equivalent weight coefficient for each ES for the temporal reference years was calculated using a revised equivalent value coefficient (Tables S1 and S2). At first, we converted the 1997 and 2007 unit values into 2017 US$ units to adjust inflation using the US Department of Labour Consumer Price Index Inflation Calculator (https://www.bls.gov/data/inflation_calculator.htm). The ESVs derived from the non-adjusted and adjusted unit values for the specific ESs are shown in Table 2. Initially, in Costanza et al. (1997) valuation, an underestimated equivalent value was approximated for cropland region that exhibited considerably lower value estimates for cropland ecosystem, which is one of the main representative ecosystem types in most of the Asian countries. Since the food production service of cropland is the most direct services we considered, and their

Table 1
Correction factors used for adjusting the model parameters.

Year	Yield	NPP	NDVI	Rainfall	FVC	NPP & NDVI
1973	1.45	1.07	1.13	1.38	2.25	1.10
1988	1.45	1.64	1.17	1.48	1.70	1.40
2003	1.32	1.54	1.26	1.54	1.55	1.40
2013	1.27	1.37	1.14	1.42	1.46	1.26
2018	1.28	1.63	1.21	1.49	1.61	1.42

valuation is entirely based on the market price, we have used these estimates as a base for the valuation of other services. After that, the equivalent value coefficient of other ESs was measured from the cropland coefficient value, assuming that the equivalent value coefficient of food production service of cropland is equaled to one (Fu et al., 2016; Song and Deng, 2017).

2.3.2. Parameter adjustment and rectification

For the regional and provincial scale, the global equivalent coefficient exhibited a substantial bias and uncertainties in valuing ESs, as it is not free from the apparent landscape complexity and spatial heterogeneity in which the given coefficients become inefficient to produce the real economic values for a target ecosystem. Several studies have adopted various factors for dynamic corrections of the value coefficient. For example, a positive association was found between amount and distribution of precipitation and water supply, water regulation services, whereas, amount of biomass, net primary productivity (NPP), and normalized difference vegetation index (NDVI) are related to GR, CR, DR, habitat generation, biodiversity maintenance, soil formation and retention services (Fu et al., 2016; Xie et al., 2008, 2017; Zhang et al., 2017; Li et al., 2018; Huang and Ma, 2013). Among those correction factors, the biomass and NPP factors were used explicitly for developing a dynamic equivalent factor and estimating indirect regulating services using a varied spatially explicit biophysical and statistical value transfer approaches (Song et al., 2015; Sannigrahi et al., 2018a,b). Additionally, studies have shown a high to a statistically significant positive correlation between the biomass-NDVI factors and ecosystem functions (Fu et al., 2016; Wang et al., 2015; Fei et al., 2018; De Groot et al., 2002). In this study, NPP, NDVI, Yield, Precipitation, fractional vegetation cover (FVC), and NPP/NDVI factors were used to adjust equivalent coefficients for several reference periods (Table 1, Fig. S1). To calculate the spatiotemporal NPP, we have used the grid level precipitation and evapotranspiration retrieved from TerraClimate (http://www.climatologylab.org/terraclimate.html; Abatzoglou et al., 2018).

Using the dynamic correction factors mentioned above, we have adjusted the corresponding equivalent value coefficient of each ESs for 1973, 1988, 2003, 2013, and 2018 reference years as follows:

$$\begin{aligned} EF_{ij} &= B_j \times F_{n1} \\ EF_{ij} &= P_j \times F_{n2} \\ EF_{ij} &= V_j \times F_{n3} \\ EF_{ij} &= Y_j \times F_{n4} \end{aligned} \tag{8}$$

where, $EF_{ij}$is dynamic equivalent factor in eco-region j and ecosystem service i; $B_j$is dynamic biomass (NPP and NDVI) correction factors for eco-region j, P_j is precipitation correction factor in eco-region j, V_j is dynamic FVC factor in eco-region j, and Y_j is spatiotemporal crop yield factor in eco-region j, F_{n1} is equivalent coefficient value of GR, CR, DR, waste treatment, pollination, biological control, habitat, raw material production, genetic resources, recreational, and cultural services, F_{n2} is equivalent coefficient value of water supply, WR services, F_{n3} is equivalent coefficient value of erosion control and soil formation services, and F_{n4} is equivalent coefficient value of food production service. The dynamic correction factors B_j, P_j, V_j, and Y_j were estimated for the entire county and administrative levels which reflects the pattern of NPP, biomass, NDVI, and rainfall at the study region and entire country as follows:

$$\begin{aligned} B_i &= \left(\frac{NDVI_i}{NDVI_j} + \frac{NPP_i}{NPP_j}\right) \\ P_i &= \left(\frac{R_i}{R_j}\right) \\ V_i &= \left(\frac{FVC_i}{FVC_j}\right) \\ Y_i &= \left(\frac{Y_i}{Y_j}\right) \end{aligned} \tag{9}$$

where, $R$and Y are rainfall and crop yield factors, i, j are the distribution of the dynamic factors at study region and the entire country scale. To estimate Y_i factor, temporal crop yield data was collected from the District Statistical Handbook, provided by the Department of Planning, Statistics, and Programme Monitoring, Government of West Bengal,

Table 2
Adjusted and non-adjusted ESVs of different land classes in the study region.

	MV		CL		CE		MA		IW		UB	
	NAD	AD	NAD	AD	NAD	AD	NAD	AD	NAD	AD	NAD	AD
GR	2	0	0	0	0	0	0	0	0	0	0	0
CR	8	6	303	215	173	125	17	12	18	13	36	26
DR	0	0	0	0	0	0	1399	1006	110	81	0	0
WR	1	0	0	0	0	0	0	0	206	166	1	1
WS	12	10	295	234	0	0	318	253	15	12	0	0
EC	9	8	79	74	9158	8540	1028	959	96	88	0	0
SF	0	0	392	370	0	0	0	0	0	0	0	0
NC	0	0	0	0	0	0	12	9	63	51	0	0
WT	16	11	292	208	0	0	42,401	30,476	111	82	0	0
POLL	7	5	16	12	0	0	0	0	0	0	0	0
BC	6	5	24	17	0	0	0	0	35	26	0	0
HA	251	184	0	0	70	50	4482	3222	90	66	0	0
FP	246	181	1712	1269	861	636	291	214	23	17	0	0
RM	11	8	161	115	4	3	94	67	20	15	0	0
GEN	251	184	768	546	65	47	81	58	4	3	0	0
REC	5	4	60	43	92	67	574	412	81	60	225	166
CUL	30	25	0	0	16	11	0	0	73	54	0	0

MV = Mixed Vegetation; CL = Cropland; CE = Coastal Estuary; MA = Mangrove; IW = Inland Wetland; UB = Urban Built-up; NAD = Non Adjusted; AD = Adjusted; GR = Gas Regulation; CR = Climate Regulation; DR = Disturbance Regulation; WR = Water Regulation; WS = Water Supply; EC = Erosion Control; SF = Soil Formation; NC = Nutrient Cycling; WT = Waste Treatment; POLL = Pollination; BC = Biological Control; HA = Habitat Service; FP = Food Production; RM = Raw Material; GEN = Genetic Service; REC = Recreation; CUL = Cultural Service.

India (http://www.wbpspm.gov.in).

Additionally, the spatiotemporal NPP using two separate models including Leith NPP (Leith 1975; 1977) and Thornthwaite Memorial (TM) model (Leith, 1977) were estimated using the following models:

$$NPP_r = 3000 \times (1 - e^{-0.000664P})$$
$$NPP_{ET} = 3000 \times (1 - e^{-0.0009695ET}) \quad (10)$$

where, NPP_r and NPP_{ET} are the Miami and TM model, r, P and ET are rainfall and evapotranspiration functions. The NDVI and FVC were estimated using the following equations:

$$NDVI = \frac{\rho_{NIR} - \rho_{Red}}{\rho_{NIR} + \rho_{Red}}$$
$$FVC = \frac{NDVI - NDVI_{\min}}{NDVI_{\max} - NDVI_{\min}} \quad (11)$$

where, $\rho_{NIR}$and ρ_{Red} are surface reflectance at near-infrared and red bands, FVC is fractional vegetation cover, $NDVI_{\max}$ and $NDVI_{\min}$ is maximum and minimum NDVI in the region (Xie et al., 2017).

2.3.3. Determining standard invariant equivalent value factor

In this study, all the four groups of ESs and functions, i.e., provisioning, regulating, supporting, and cultural services were incorporated to measure the per unit ESVs using the corresponding equivalent value (EV) and a modified equivalent value factors (EVF) approximated for the selected ESs (Xie et al., 2017; Costanza et al., 2017; Song and Deng, 2017; Xie et al., 2008). The EVF is a simplistic approach and requires less extensive data. It is the easiest way to measure the EV of ecosystem types and services. Here, we have analyzed total 17 ESs and functions proposed by Costanza et al. (1997, 2014) and De Groot et al. (2012) to quantify the spatiotemporal ESVs using a revised EVF for five reference years. Additionally, we have evaluated the spatiotemporal variation and response of these ESs to LULC changes for seven major eco-regions of Sundarbans, i.e., cropland, mangrove, natural vegetation, coastal estuary, inland wetland, sandy coast, and urban land, respectively. Song and Deng (2017) reported that in Costanza et al. (1997) valuation framework which is based on simple benefit transfer approach, the cropland ecosystem had been excluded from assigning per unit EV for any ESs, assuming that this ecosystem has no specific contribution towards the provision of ESs, except food production service. This may be due to the per unit EV of major ecosystem types of the world was initially approximated for the western countries, where agriculture system appears to be insignificant to produce valuable ESs. Moreover, an underestimated EV of cropland compare to other ecosystems is the main reason of undervalued ESV in the agriculture-based nations, especially in India, where farmland is one of the most significant ecosystem types (Sannigrahi et al., 2018a,b). In this study, we adopted the updated per unit values provided by Costanza et al., (2017) and De Groot et al. (2012), and subsequently the per unit equivalent value was measured from the cropland equivalent value. Initially, the equivalent value coefficient of food production service of cropland was chosen one. Afterward, the equivalent weight factors of the remaining ESs were calculated from the cropland equivalent factor. Additionally, depending on the average crop production statistics of the study region, we have estimated the average food production value of cropland assuming that the proposed food production is equal to 1/7 of the actual food production. Later, the equivalent value of food production service for per unit area of cropland and other ecosystems were estimated by multiplying the EV and corresponding equivalent weight coefficient. Moreover, using the equivalent value of food production service of cropland (Liu et al., 2010; Xie et al., 2003, 2008), the equivalent value of the remaining services and functions were calculated (Fu et al., 2016). The economic value of food production service of cropland was measured as:

$$E_a = 1/7 \left(\sum_{i=1}^{n} (P_i \times Q_i) \right) \quad (12)$$

where, E_a is the economic value of food production service provided by cropland (US$ ha^{-1}), i is the crop types, P_i is the price of the crop i (US$ kg^{-1}), and Q_i is yield of the crop i (Kg ha^{-1}). Additionally, using the crop price (0.27 US$ kg^{-1}) and crop yield (2458.85 kg ha^{-1}) of major crops of the study region, the equivalent value of food production of cropland was estimated 94.55 US$ ha^{-1}. This dynamic equivalent value was adjusted with inflation factor.

2.3.4. Dynamic correction and invariant/comparable economic valuation

In the time series ES valuation, it is essential to adjust the data for confirming the comparability of economic estimates and to develop a standard invariant equivalent value by eliminating the price fluctuation, inflation, and fixing other economic factors. Different economic indicators including the Purchasing Power Parity (PPP), Consumer Price Index (CPI), Willingness to Pay (WP), inflation rate, Engel coefficient (En), Pearl growth curve model, etc. have been used extensively to standardize economic values at regional and local scale ESV estimation. Here, we first estimated the comparable economic value of food production service of cropland utilizing the information of the inflation index as follows:

$$E_{an} = E_{am} \times \frac{\phi_m}{\phi_n} \times 100\% \quad (13)$$

where, E_{an} is invariant economic value, E_{am} is the current economic value of food production service of cropland ecosystem in the year m, ϕ is the yearly inflation index, m, n is current and past year. The inflation index can be calculated as follows:

$$IR = \frac{CPI_m - CPI_n}{CPI_n} \times 100 \quad (14)$$

where $IR$is the inflation rate, $CPI$is consumer price index, m, n is current and past year.

The level of socio-economic development and awareness of people about the need for ESs significantly determine the economic values of ESs, especially the indirect ecosystem goods and services (De Groot et al., 2002). Several approaches including the willingness to pay, willingness to accept, hedonic pricing, Pearl's S-shaped growth curve (PGC) model have been utilized explicitly to evaluate the impact of human development on economic valuation of ESs. The awareness and people's willingness to pay is determined by the “S” shape pattern of socio-economic development (Fu et al., 2016). The awareness would be low at the lower stage of socio-economic development and vice versa. In this study, we have used the PGC model to assess the linkages between the level of socio-economic development and ESs as follows:

$$E = \frac{1}{1 + e^{-t}} \times E_{an} \quad (15)$$

$$t = \frac{1}{E_n} - 3 \quad (16)$$

where E is the adjusted ESV in the year m, e is natural logarithm, t is socio-economic development indicator, E_{an} is food production service value of cropland in the current year, E_n is Engel coefficient ranges between 0 and and 1.

2.3.5. Estimating regional ecosystem service values using adjusted coefficient

Using the adjusted unit values, we have measured ESVs of seven ecosystems of Sundarbans for five reference years. We also calculated the spatiotemporal distribution and changes of ESV's during five reference periods, i.e., 1973–1988, 1988–2003, 2003–2013, 2013–2018, and 1973–2018. The total ESV's was calculated as follows:

$$ESV_j = \sum_{i=1}^{17} E \times EF_{ij} \times A_j \quad (17)$$

$$ESV_i = \sum_{j}^{7} E \times EF_{ij} \times A_j \quad (18)$$

$$ESV = \sum_{i=1}^{17} \sum_{j=1}^{7} E \times EF_{ij} \times A_j \quad (19)$$

where, ESV_j, ESV_i, and ESV is ecosystem service value (US$ ha^{-1} year^{-1}) of ecosystem type j, and ecosystem service i, total ecosystem service value, E is dynamic corrected food production service of cropland (US$ ha^{-1}), EF_{ij} is the dynamic adjusted equivalent value coefficient of ecosystem service i and ecosystem types$j$, A_j is area (ha) of ecosystem type j, respectively (Kindu et al., 2016; Liu et al., 2012; Costanza et al., 2017; Yoshida et al., 2010; Yushanjiang et al., 2018). After that, the spatiotemporal change rate and dynamic degree of changes of ESV were measured as follows:

$$\Delta ESV_{ij}(\%) = \frac{ESV_{end} - ESV_{start}}{ESV_{start}} \times 100\% \quad (20)$$

$$\Delta ESV_{ij} = \frac{ESV_{end} - ESV_{start}}{ESV_{start}} \times \frac{1}{t} \times 100\% \quad (21)$$

where ΔESV_{ij}refers to the change of ESV's of ecosystem type j and ecosystem services i ESV_{end} and ESV_{start} exhibits the ESV of past and current year of the research period, t represent the periods, respectively.

2.4. Estimating coefficient of sensitivity, the coefficient of elasticity, ecosystem service sensitivity index, and coordination degree

To measure the impact of any external disturbances on ESs, there is a need to perform a sensitivity test, therefore, we have tested four different sensitivity tests including the Coefficient of Sensitivity (CS), Coefficient of Elasticity (C_{ES}), ecosystem service sensitivity index (ESSI), and Coordination Degree (CD) for different reference years and periods. The CS is based on a standard economic concept of elasticity, was used for assessing the impact of LULC changes on ESs, measured as follows:

$$CS = \frac{(\mathrm{ESV}_j - ESV_i)/\mathrm{ESV}_i}{(VC_{jk} - VC_{ik})/\mathrm{VC}_{ik}} \quad (22)$$

where ESV refers to ecosystem service value, VC is value coefficient, $_i$ and $_j$ represent initial and adjusted values, and k is ecosystem types. Additionally, the spatiotemporal stationarity and changes of ESV is measured through variation of VC, as ESV measured for each ecosystem types and services would be elastic when CS exceeds the threshold (> 1). Also, the value would be inelastic when CS < 1. In addition, CS = 1 and CS = 0 indicates the complete (in)elasticity (Fu et al., 2016; Tolessa et al., 2017; Yi et al., 2017; Sannigrahi et al., 2018a,b). This signifies that the use of an accurate ecosystem value coefficient would be more critical when high relative proportional changes in VC is associated with high proportional changes in ESV (Kreuter et al., 2001). Additionally, we have framed five different value coefficient degree, i.e., 50%, 40%, 30%, 20%, and 10% to assess the sensitivity of ESV's at different value coefficient level.

The coefficient of elasticity (C_{ES}) depicts the sensitivity of a responding variable to change one control variable (Sannigrahi et al., 2018a,b; Song and Deng, 2017). In this study, we measured ES elasticity of the major ecosystem types and services of Sundarbans using spatiotemporal LULC change as a control variable and per unit changes of selected ESs as a response variable. These estimates would be helpful to categorize the most vulnerable and distressed ecosystem at any given ecosystem. The C_{ES} was measured as follows:

$$C_{ES} = \frac{((ESV_i - ESV_j)/ESV_j) \times 100\%}{LCP} \quad (23)$$

$$LCP = \frac{\sum_{i=1}^{7} TA_j}{\sum_{i=1}^{7} A_j} \times \frac{1}{t} \times 100\% \quad (24)$$

where, ESV_i and ESV_j is the end and the start of the research period, LCP is the land change percentage, TA is converted area of ecosystem type j, A_j is the area of ecosystem type j, t is research period. Additionally, we have identified the most sensitive ecosystem of the region using both coefficients of elasticity for a reference period and coefficient of sensitivity of the starting and end of the research periods. Moreover, to evaluate association and coordination between the changes of ecosystem types and ESVs, temporal coordination degree (Luo et al., 2018) was measured using the following equation:

$$CD = \frac{\Delta L_{tj}/L_{tj-1}}{\Delta E_{tj}/E_{tj-1}} \times 100 \quad (25)$$

where $\Delta L_{tj} = L_t - L_{t1}$, $\Delta E_{tj} = E_t - E_{t1}$ L_{tj} is the area of ecosystem type j in the year t, L_{tj-1} is the area of ecosystem type j in the year $t-1$, E_{tj} is ecosystem service value of ecosystem type j in the year t, E_{tj-1} is ESV of ecosystem type j in a year $t-1$.

2.5. Evaluating spatial scale-dependent synergies and trade-offs of ecosystem services

Spatial scale-dependent trade-offs and synergy among the ESs were evaluated at multiple spatial scales. The trade-off is a situation when the uses of one ES directly or indirectly decrease another ES. Therefore, it is based on win-lose or lose-win situation. The synergy is a situation when uses of one ES is increasing benefits of another ES, and thereby produce a win-win situation. Using ArcGIS fishnet tool, 20 spatial grids starting from 1 km to 20 km were prepared, and the average value was taken for each grid. The grid data were normalized in a range between 0 and 1 eliminating effects of outliers during model construction. Total 68,240, 16,699, 7,306, 4,004, 2,535, 1,735, 1,238, 912, 707, 568, 462, 374, 310, 254, 232, 185, 170, 134, 126, and 114 samples were extracted and used for grid-scale analysis for 1 km–20 km grid size. Zonal mean values of two administrative divisions, including the block level and county level, were adopted for estimating spatial trade-offs and synergies. Moreover, the spatial correlation between all four ES bundles (regulating, supporting, provisioning, and cultural) was measured through a per pixel analysis using the ArcPy site-packages. PerformanceAnalytics packages in R statistical software measured Pearson correlation matrix across the scales.

3. Results

3.1. Classification and spatiotemporal changes of LULC (1973–2018)

Cropland is the dominant land use type in the study region, contributing 44.8% to the total geographical area, followed by coastal estuary (21.95%), mangrove forest (15.9%), mixed vegetation (12.57%), urban built-up (2.38%), inland wetland (2.24%), and sandy coast (0.11%) (Fig. 2a and b). The coastal estuary, mangrove, and inland wetland ecosystems are the most important and ecologically and biologically diverse ecosystems in the study region and have increased in the geographical extent between 1973 and 2018 (Fig. 2a and b). The spatial conversion of the LULC classes is presented in Fig. S2 and Fig. S3. During 1973–2018, urban land has significantly increased at the expense of cropland and greenspace in and around the Kolkata suburbs. The inland water bodies also increased during this period at the expense of cropland and natural green cover. A significant area of mangrove cover is lost during the study period, primarily due to coastal erosion and human-led destruction.

The performance and accuracy of machine learning models were

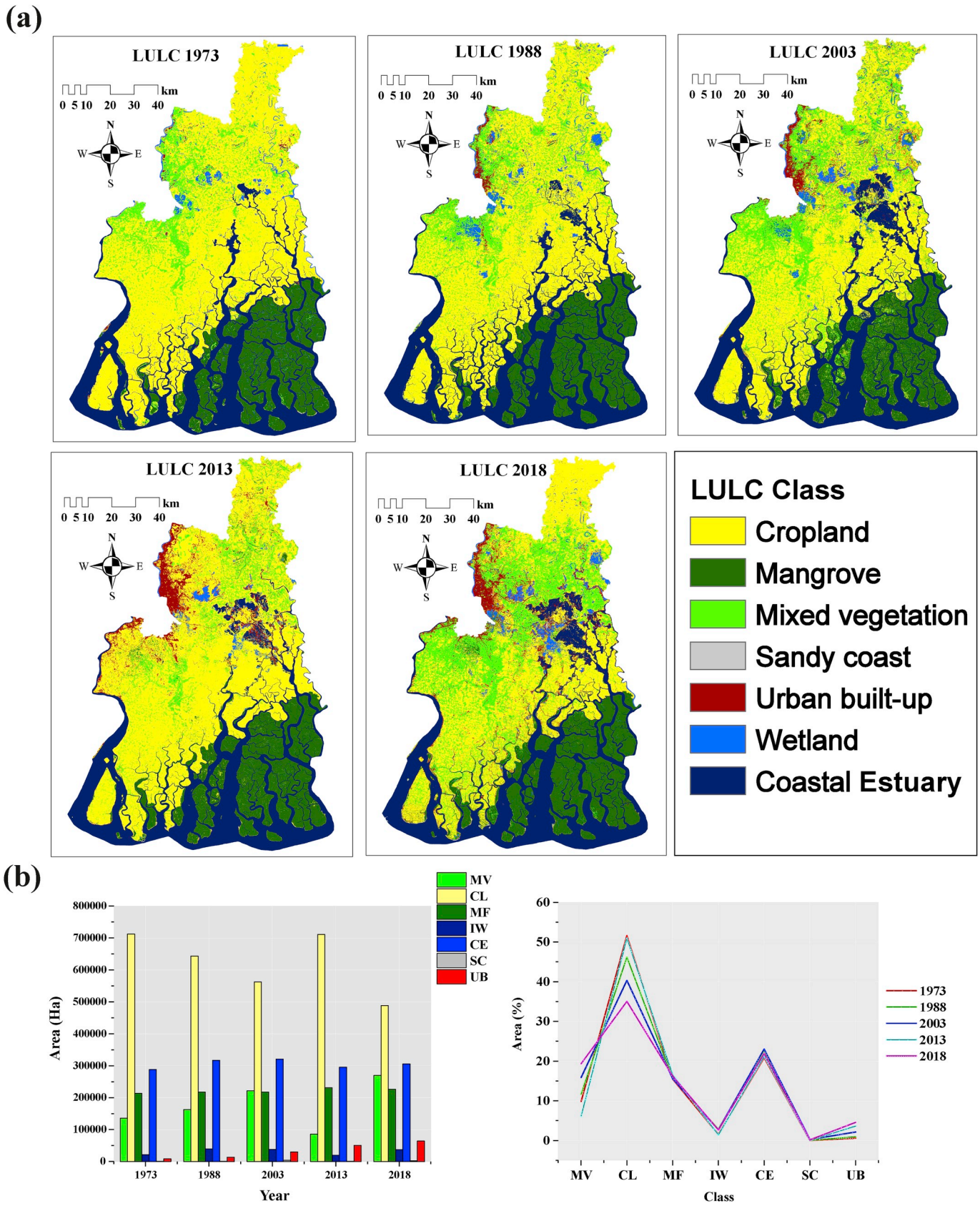

Fig. 2. **(a)** Distribution of the major land use land cover types of Sundarban estimated for five reference years, **(b)** shows the area (ha) and proportion (%) of the eco-region.

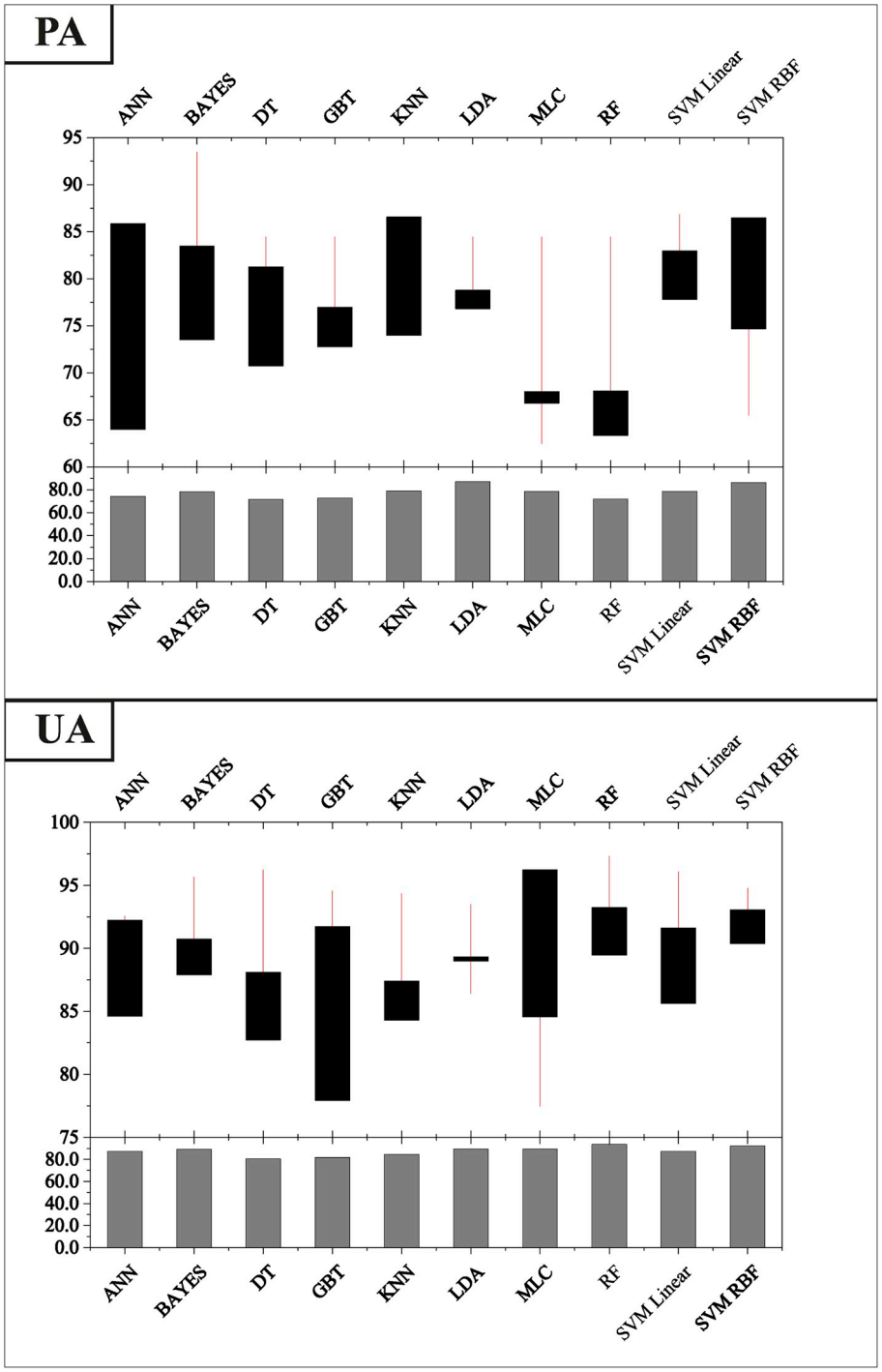

Fig. 3. The producer's accuracy (PA) and user's accuracy (UA) of the ten supervised models.

assessed through an area based unbiased approach including UA, PA, OA, and Kappa statistics (Tables S3 and S4, Fig. 3). For all the study years, MLC algorithm has exhibited the least accuracy, except for the year 1973. Among the ten machine learning models, RF and SVM performed the most accurate for all the reference years (Table S3). Considering the other two statistics namely OA and Kappa, the best results were obtained for RF and SVM models (Fig. 3, Table S4). SD value was found to be the highest for MLC model, followed by LDA, RF, DT, ANN, GBT, BAYES, KNN, SVM, and SVMLIN, respectively Fig. 4). The lower SD value indicates the high model performances and the least uncertainty. The GC is a similar measure to assess the spatial association between the models used for LULC classification. The highest GC value was found for SVMLIN, followed by SVM-RBF, KNN, ANN, GBT, BAYES, DT, RF, LDA, and MLC (Fig. 4). High GC values are equivalent to high model performances and least uncertainty. Thus, the SVMLIN and SVM-RBF were found to be the best algorithms to perform supervised classification. The maximum overall CS value was found for ANN for all reference years, followed by RF, SVMLIN, KNN, DT, LDA, BAYES, SVM-RBF, GBT, and MLC. The PA test was also performed to assess spatial agreement between two supervised models. Maximum PA value was found for SVMLIN, followed by SVM-RBF, ANN, KNN, GBT, BAYES, RF, DT, LDA, and MLC. Furthermore, we have conducted the BCD test to examine dissimilarity between the models. High BCD values are representing the least model accuracy and high uncertainties in

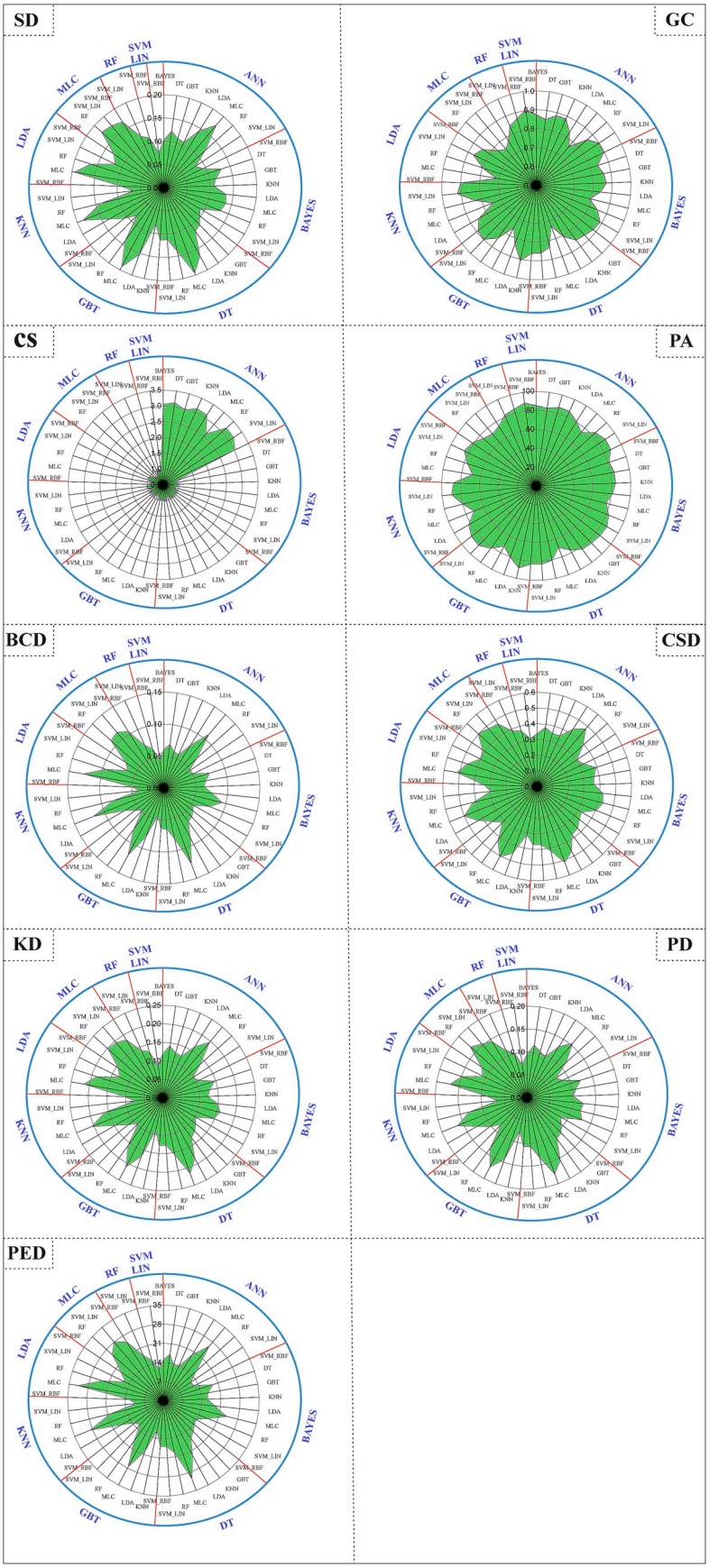

Fig. 4. Similarity and dissimilarity statistics between the land use land cover classification derived from 10 machine learning models. SD = Spearman Dissimilarity, GC = Gower Coefficient, CS = Cosine Similarity, PA = Percent of Agreement, BCD = Bray Curtis Distance, CSD = Chi-Square Dissimilarity, KD = Kendall Dissimilarity, PD = Pearson Dissimilarity, PED = Percent of Disagreement.

model estimates. Additionally, the CSD test was performed to evaluate spatial homogeneity of the models and suggests that among the ten algorithms, the SVM performs most accurately. The results of the KD test, conducted to assess the model, indicates the least accuracy and high uncertainty and dissimilarity. Among the ten machine learning algorithms, the highest KD value was found for MLC, followed by LDA, RF, DT, GBT, ANN, BAYES, KNN, SVM-RBF, and SVMLIN. The PD test was used to test the spatial dissimilarity between the models. High PD reflects high spatial dissimilarity and vice-versa. PED test was used to examine the percent of disagreement between the models. High PED value indicates more substantial uncertainty and least model performances. In this analysis, we found high PED value for MLC, followed by LDA, DT, RF, BAYES, GBT, KNN, ANN, SVM-RBF, and SVMLIN, respectively (Fig. 4).

3.2. Spatiotemporal variation of correction factors

Table 1 shows temporal variation of the six correction factors (yield, NPP, NDVI, rainfall, FVC, and NPP & NDVI) used to adjust the global value coefficients for estimating the spatially explicit value of multiple key ESs for the study period. Yield factor was varied from 1.27 to 1.45, found the lowest in 2013 (1.27) and the highest (1.45) in 1973 and 1988. NPP value was minimum (1.07) in 1973 and a maximum (1.64) in 1988. NDVI value reached maximum (1.26) in 2003 and a minimum (1.13) in 1973, respectively. The FVC estimates were found the highest (2.25) in 1973 and the lowest (1.46) in 2013 during the study periods. Additionally, it has been observed that the maximum (1.42) and minimum (1.10) NPP & NDVI value was attained in 2018 and 1973 (Table 1).

Fig. 5 and Figs. S4 and S5 show the spatiotemporal variation of monthly NPP derived from two NPP models, i.e., Miami and TM. Miami NPP (gC m^{-2} $month^{-1}$) ranges from ≈0 in January to ≈500 in Jun-July-August, depending on the variation of monthly precipitation which was used as a slope factor to estimate Miami NPP for the studied period. The TM NPP, which is based on the monthly variation of evapotranspiration, was found maximum value (≈380) in May, and minimum value (≈110) in January. The highest average NPP of Sundarbans was measured (≈450) during the monsoon period (Jun, July, August) and the minimum (≈50) is recorded during the post-monsoon period (December, January, February). The optimum climatic, bioclimatic, phenological, and environmental stress variables including the maximum and minimum temperature, precipitation, photosynthetically active radiation (PAR), fraction of photosynthetically active radiation (fPAR), NDVI, EVI, temperature stress, and water stress was found during the post-monsoon season. Thereby the peak NPP values were found in the post-monsoon season. More details are given in the discussion section.

3.3. Spatiotemporal variation and changes in ecosystem service values

Figs. 6 and 7 shows the spatial and temporal distribution and changes of ESVs for five reference years, i.e., 1973, 1988, 2003, 2013, and 2018. The highest ESVs (million US$ $year^{-1}$) was observed over the Gosaba, and Kultali block in Sundarbans. Open and dense mangrove forests mainly cover these administrative provinces. Furthermore, due to the expansion of water bodies including inland wetland and estuarine surface, the total ESV's were increased during the study period. These changes of ESVs (both positive and negative) are the outcomes of land degradation and conversion of productive land into semi-modified and artificial land.

In all reference years, the maximum ESV (both non-adjusted and adjusted, million US$ $year^{-1}$) is produced by mangrove forest, followed by the coastal estuary, cropland, inland wetland, mixed vegetation, and urban land, respectively (Fig. 8a). Considering the temporal changes of ESVs during 1973–2018, mangrove ESV has increased significantly, followed by mixed forest, inland wetland, and urban land, whereas, the coastal estuary and cropland ESVs have decreased in the last 45 years.

Among the ES's, the WT service is the main ES of SBR with maximum (un)adjusted ESV (million US$ $year^{-1}$), followed by EC, HA, FP, DR, GEN, SF, WS, REC, CR, RM, WR, CUL, NC, BC, and POLL. (Fig. 8b, Table 2). During the entire research period (1973–2018), the ESV of EC has declined most rapidly, while a moderate to a low declining trend is observed for FP, SF and WS services. During this period, a positive change of ESVs was noted for WT, followed by HA, REC, DR, GEN, WR, CR, CUL, NC, RM, BC, and POLL services. The increase of the key regulating and supporting services is attributed to the expansion of mangrove and water bodies during the study period. Additionally, the rise in inland waterbodies at the expense of cropland and natural green surface is evident in this research. This trend is evident in and around the Sandeshkhali, Canning, Minakhan, Haora administrative province due to higher involvement of shrimp cultivation and associated practices. In contrast, we observed that significant crop areas are lost during this study period. This could be the reason for declining provisioning services in Sundarbans, which is one of the primary sources of livelihoods of the residents of Sundarbans (Table 2). The cropland ecosystem is necessary for the production of food production service, which is the main provisioning services considered in this study. Except for Gosaba and Kultali blocks (covered by dense mangrove forest), most of the administrative blocks of Sundarbans is characterized by high crop yield and production. The declining status of the food production service resembles a serious socio-economic threat to the communities live and reliant on the natural agricultural commodities and associated economic activities. The mangrove ecosystem is providing the multiple key ESs including WT, HA, DR, EC services, etc. The inland wetland ecosystem is exceptionally beneficial in producing the WR, EC, DR, WT, HA

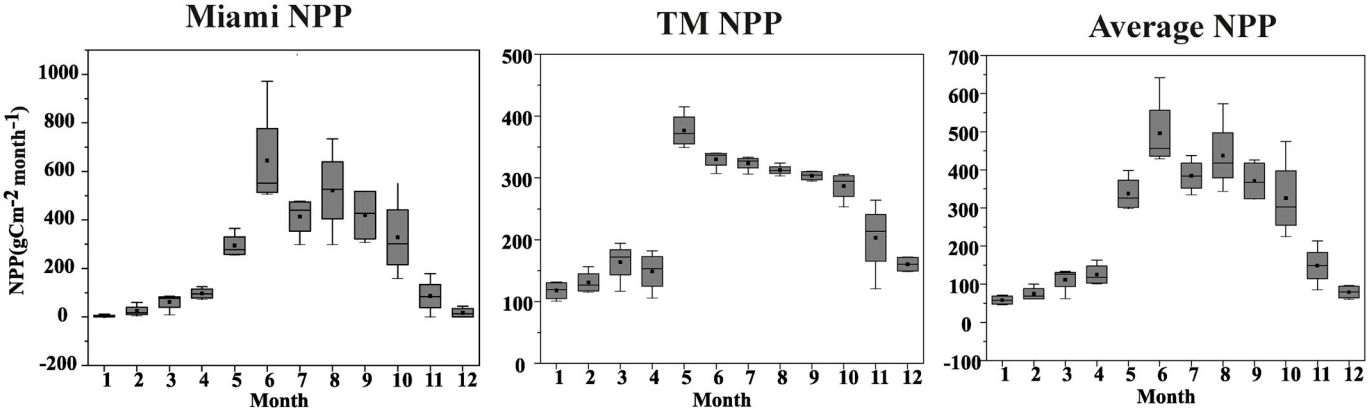

Fig. 5. Monthly variation of Miami NPP (gC m^{-2} $month^{-1}$), Thornthwaite Memorial (TM) NPP (gC m^{-2} $month^{-1}$), and average NPP (gC m^{-2} $month^{-1}$) during the study period.

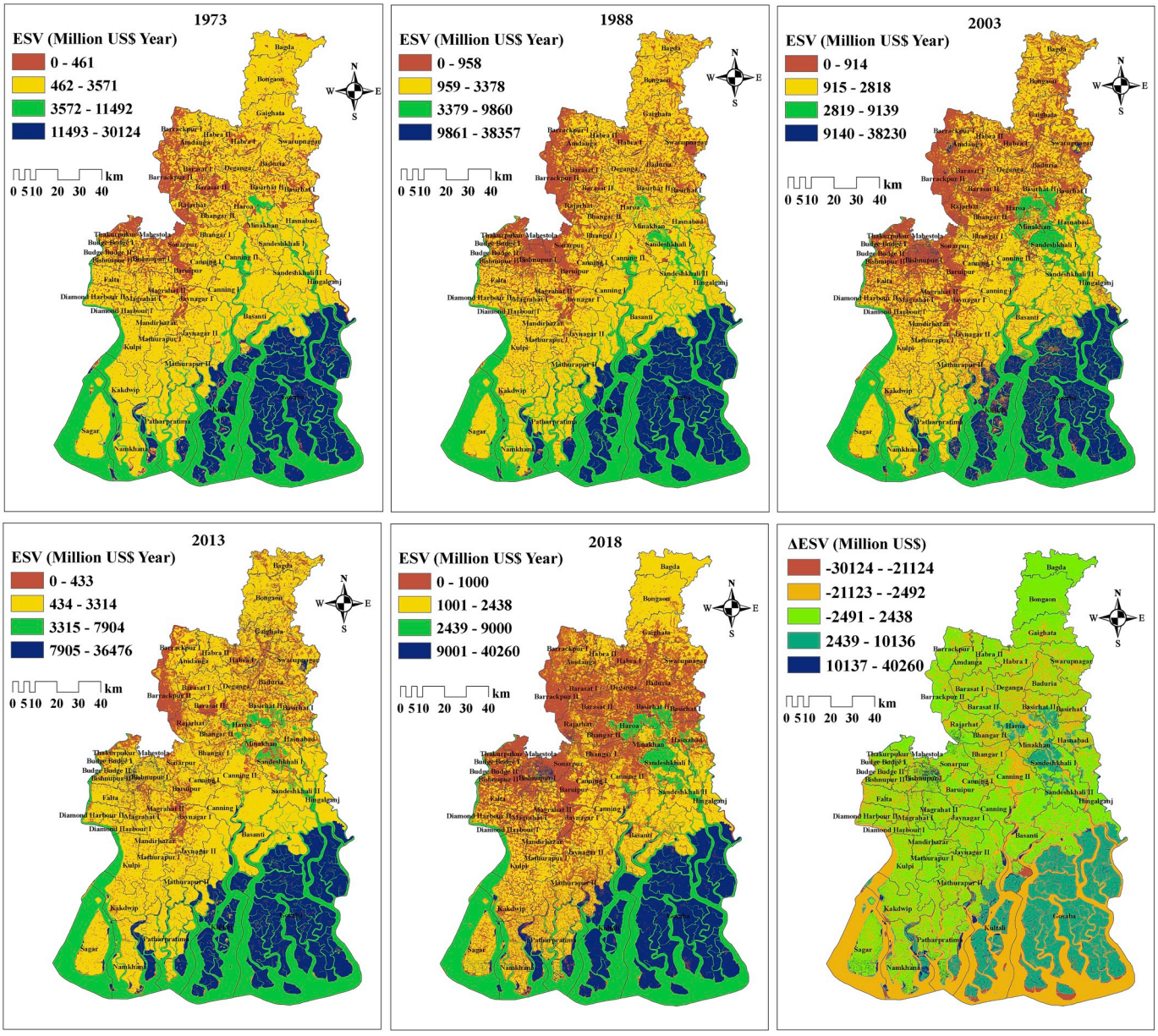

Fig. 6. Spatial distribution of ESVs (Million US$ year^{-1}) in 1973, 1988, 2003, 2013, 2018, and during the entire research period.

and REC services (Table 2). However, due to the significant increases in ecologically productive lands, the net changes of ESV's were found positive during the research period (Fig. 8c). This exhibits the environmental stability of the ecoregions.

3.4. Sensitivity and elasticity of ecosystem service values to land use changes

To understand the level sensitivity of ESVs at different land use and value coefficient scenarios, the CS was measured for five sensitivity levels (50%, 40%, 30%, 20%, and 10%) (Fig. 9a and b). Among the ecosystem types, mangroves are the most sensitive to any anthropogenic changes, followed by the coastal estuary, cropland, mixed vegetation, and inland wetland, respectively.

To evaluate the sensitivity of each ES's to LULC changes, we performed the sensitivity test for the 17 major ESs for five reference years (Fig. 9c and d). Among the 17 ESs, the WT service was found most sensitive for all sensitivity level, followed by EC, HA, FP, DR, GR, SFR, WS, REC, CR, RMP, WR, CUL, BC, NC, and POL services, respectively. This provides an insight to understand the response behavior of the key ESs to LULC changes, and this could be helpful for long-term land use planning and sustainable natural resource management. Fig. 10a shows the changes of ESVs to one unit change of LULC for different reference years. During the entire research period (1973–2018), a negative elasticity value was documented for cropland and coastal estuary, whereas, the remaining ecosystems have produced low to very high elasticity to LULC changes. Fig. 10b shows the elasticity status of the selected ESs for five reference periods. During the entire research period (1973–2018), the SF, EC, FP, and WS services exhibited negative elasticity values, and CUL, REC, WR, NC, BC, HA, DR, WT, POLL, CR, GEN, and RM services showed high to low positive elasticity to LULC changes. This suggests the improving status of regulating and supporting ESs in the survey period; however, a very negative elasticity observed for FP, SF, EC services indicate the decreasing status of the provisioning services in Sundarbans.

In this study, we have performed a new test called ESSI by combining two sensitivity assessments (coefficient of sensitivity and elasticity), to identify the most sensitive ecoregions of Sundarbans (Fig. 10c). During research periods (1973–2018), mangrove was found

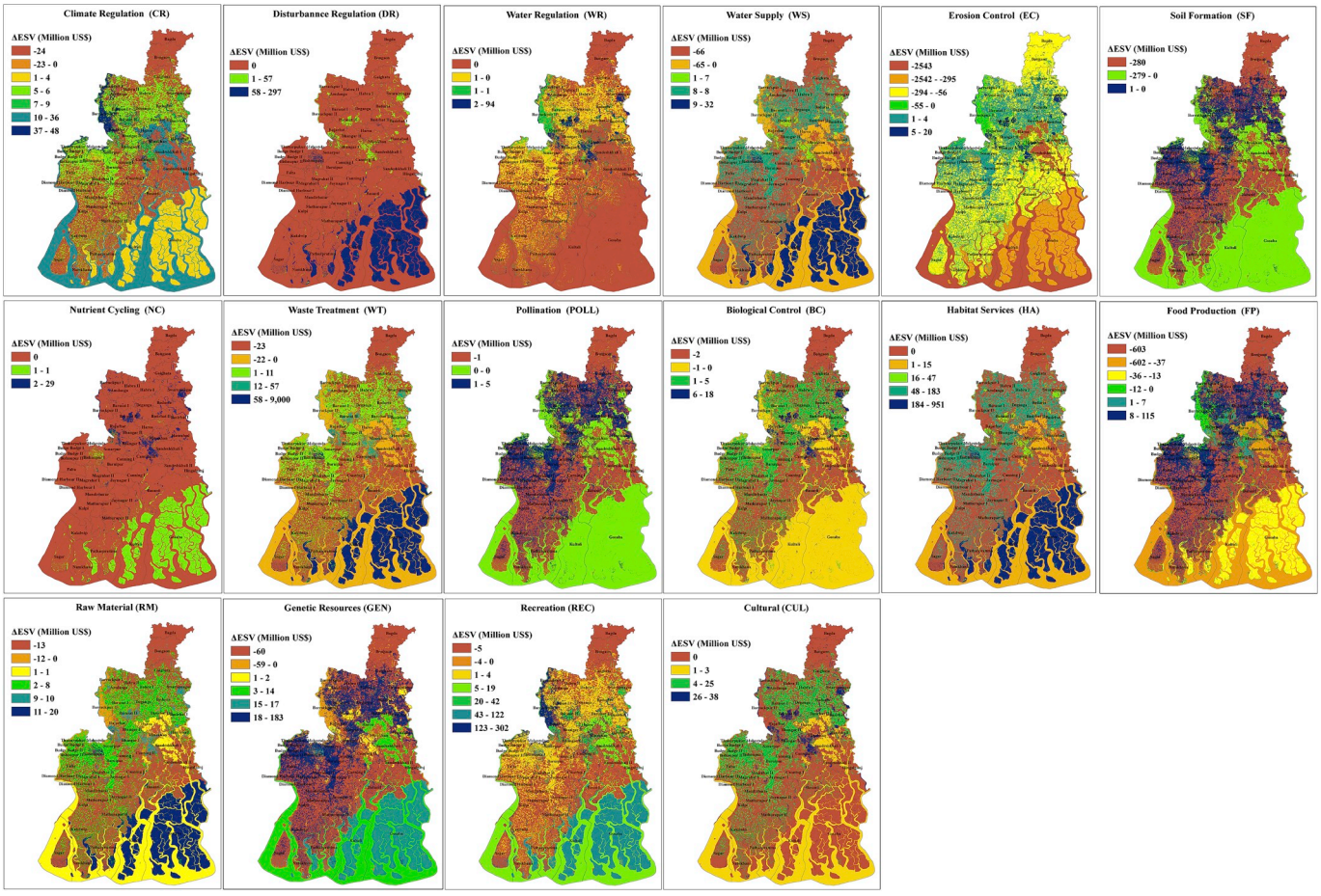

Fig. 7. Spatiotemporal changes of the ESs during the study period (1973–2018).

to be the most sensitive ecosystem with the highest ESSI value, followed by inland wetland, mixed vegetation, coastal estuary, and cropland, respectively. The outcome of this estimate could be used as an addition to the conventional sensitivity measures where both the ESV coefficient and land use fluctuation would play a significant role in identifying the most sensitive and vulnerable ecoregion at any given ecosystem.

Additionally, we have performed another test to examine the coordination between the ESs and LULC changes at multiple reference periods (Fig. 11). The high and low coordination degree (CD) represents higher and lower degree of association between ESs and LULC changes. The outcome of this test could be helpful to understand the nature and sensitivity of different ESs to any external forces. Due to the subtle decline of provisioning services during the research periods, we have observed a sharp positive association between the declining cropping area and cropland ESVs for all reference periods. This suggests that the cropland ESV appears to be most vulnerable due to substantial decreases of cropping area at the expense of shrimp pond, mixed vegetation, and urban land.

3.5. Trade-offs and synergies among the ESs at multiple scales and reference years

To understand trade-offs (negative association) and synergies (positive association) between the bundles of ESs, we have performed a spatial correlation test between the four major bundles of ESs (Fig. 12). A very high synergy was found between the provisioning and cultural services over the cropland region. While a trade-off relation observed between provisioning and cultural services over the coastal estuary, inland wetland, and urban area depicts a negative relationship. The coastal estuary and inland wetland have no such capability to produce substantial provisioning services, and hence, exhibiting a trade-off association during the research periods. A very high synergy was observed between provisioning and regulating services. While analyzing provisioning and supporting services, a moderate to strong synergies were measured over the coastal estuary and urban region, while a medium to very high synergy was measured for inland wetland ecosystem. For regulating and cultural services, a moderate to strong synergies are documented for coastal estuary and cropland ecosystem, and low to very high trade-offs is evident for mixed vegetation, urban land, and inland wetland region. Also, for regulating and supporting services, a moderate to very high synergies were reported for coastal estuary, urban land, and partly for mixed vegetation. This trend was reversed for inland wetland and mixed vegetation classes, where a moderate to strong trade-offs are evident between the regulating and supporting ESs. While evaluating the spatial association between supporting and cultural ESs, a very high to moderate trade-offs were observed for coastal estuary and urban areas, whereas, low to strong synergies are documented for mixed vegetation and inland wetland system.

To assess the effects of spatial scale on trade-offs and synergies among the ESs, we have performed the Pearson correlation test at multiple spatial scale including grid scale, administrative (block) scale, and county scale (Fig. 13a and b, Fig. S6, and Table S5). At the administrative scale, a statistically significant association (both trade-off and synergy) was found between WT and WS, WS and WR with REC, WS and WR with DR, WR and BC, NC and EC, HA and CUL, EC and CR, and DR and CUL (Fig. 13a, Fig. S6). At county scale, only three pairs are found significant at the $p \leq 0.001$ level, five pairs were significant at

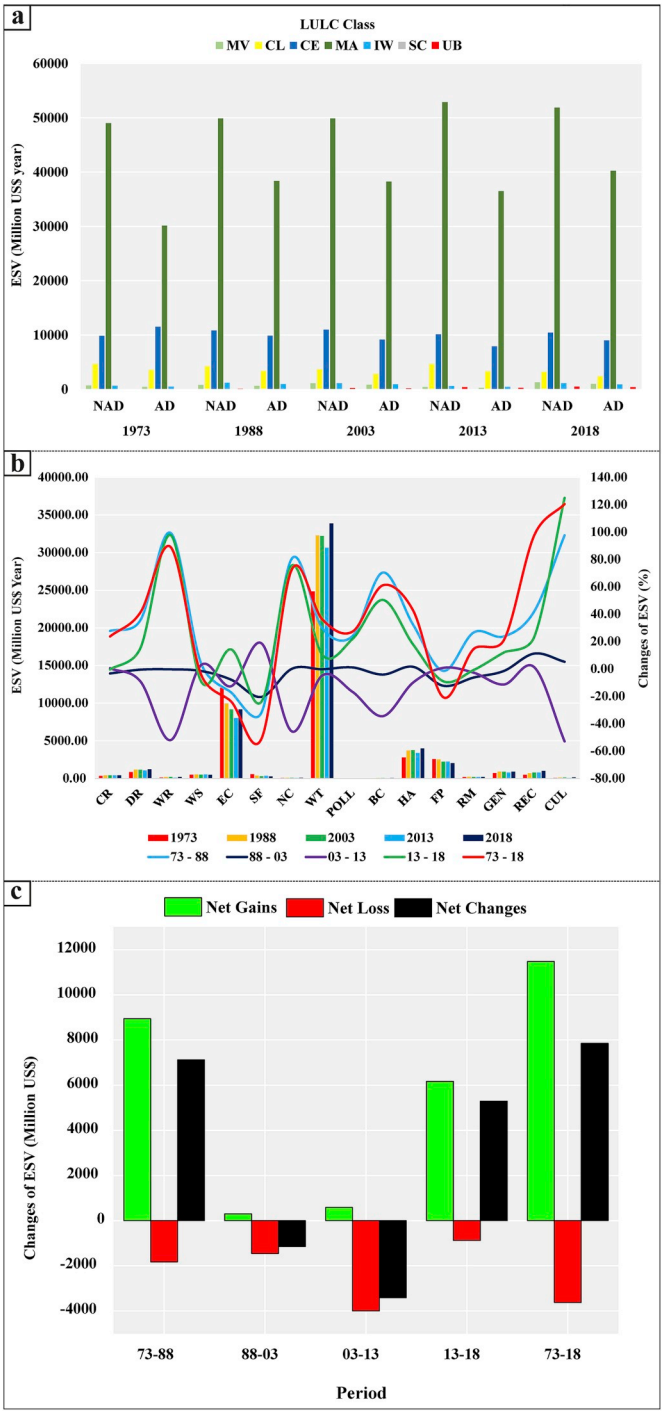

Fig. 8. (a) Shows the ESVs (Million US$ year^{-1}) of the major ecosystem types of the study region for five reference years, **(b)** shows the ESVs (Million US$ year^{-1}) of the selected ESs for five reference years, **(c)** shows the met gain, net loss, and net changes of ESVs during 1973–1988, 1988–2003, 2003–2013, 2013–2018, and 1973–2018. NAD = Not Adjusted, AD = Adjusted. MV = Mixed Vegetation, CL = Cropland, CE = Coastal Estuary, MA = Mangrove, IW-Inland Wetland, SC = Sandy Coast, UB = Urban Built-up region.

$p \leq 0.01$ level and total 33 number of pairs are found to be significant at $p \leq 0.05$ level. Additionally, at the county scale, total 79 pairs didn't exhibit any significant correlation.

4. Discussion

4.1. Linkages between LULC and ESV change

For evaluating the uniformity of our LULC classification, we compared our results with several other studies for the same ecosystem. Nandy and Kushwaha (2010) had estimated the area of different mangrove categories including Avicennia, Phoenix, mixed mangrove, mangrove scrub, etc. together shared ~223,400 ha geographical area in 2002, which is much closer to our estimates of 217,685 ha for 2003. Akhand et al. (2017) conducted a thorough time-series evaluation to estimate the changes of mangrove cover of Indian Sundarbans for four reference years 1975, 1989, 2001, and 2013 using multi-source remote sensing products. This study revealed that the mangrove covers in 1973 were 222,400 ha, which reduced to 216,500 ha in 1989, 215,300 ha in 2001, and 211,700 in 2013. In our study, we have estimated 213,791 ha mangrove forest cover in 1973, 217,541 ha in 1988, 217,685 ha in 2003, 230,833 ha in 2013, respectively. Also, for the mentioned reference years, we had approximated a negligible under/overestimated mangrove cover than that of the Akhand et al. (2017) estimation. Datta and Deb (2012) revealed that during 1975–2006, open mangrove ecosystem was severely affected due to an acute demand for cropland and hence resulted in the transformation of mangrove to cropland, and shrimp pond due to increasing demand for brackish water aquaculture (Fig. S3). However, on the contrary, the dense mangrove cover has increased in this period which is in accordance with our observation. In additional to these, Giri et al. (2007) studies on dynamics of mangrove covers in Indian Sundarbans and reported that during 1970–2000, mangrove cover of Sundarbans decreased by 1.2%, whereas, near the same period (1973–2003), our study reported an increasing mangrove area by 0.12%, derived from the results of 10 most sophisticated machine learning algorithms. However, the study by Giri et al. (2007) stated that the mentioned estimation could be a result of erroneous classification, which can be due to the variation of the tide, when most of the intertidal features including tidal flat, mud flats, small water channels are often exhibiting a similar spectral signature. Additionally, Giri et al., 2011 reported dynamics of global mangrove had revealed that except 20° N to 25° N, (the Sundarban mangrove ecosystem is located in this zone), the mangrove ecoregion is decreasing gradually with the increase in latitude. When the global mangrove areas followed a decremental trend, the Sundarban mangrove has not changed substantially, despite having multiple physical and anthropogenic disturbances (Giri et al., 2011).

Due to the increase of productive land, a net gain of ESVs was measured as 7855 million US$ during 1973–2018 (Fig. 6). For each ecosystem, the ESV (million US$ year^{-1}) of mixed vegetation, cropland, coastal estuary, mangrove, inland wetland, and urban built-up region categories varied from 39 in 1973 to 40,260 in 2018. The maximum ESV is reported for mangrove ecosystem, followed by coastal estuary, cropland, inland wetland, mixed vegetation, and urban land depicting the importance of natural ecosystems primary correspondence to mangroves and waterbodies (both freshwater and coastal wetland) in order to produce the key ecosystem goods and services which are indispensable for human well-being and subsistence (Costanza et al., 2017; MEA (Millennium Ecosystem Assessment), 2005; De Groot et al., 2012, Keesstra et al., 2018). Additionally, the mangrove-rich Sundarbans are providing a substantial ESV for the key regulating services including DR, WR, EC, where coastal floods, cyclone, coastal erosion, salinization are exhibiting serious environmental, socio-economic threats to coastal communities of Sundarbans.

4.2. Spatial scale dependent trade-offs and synergies

LULC change is the outcome of various human or natural actions, which vary from local to regional scale in dimension and direction. The spatial association among the ESs and the effects of LULC changes on

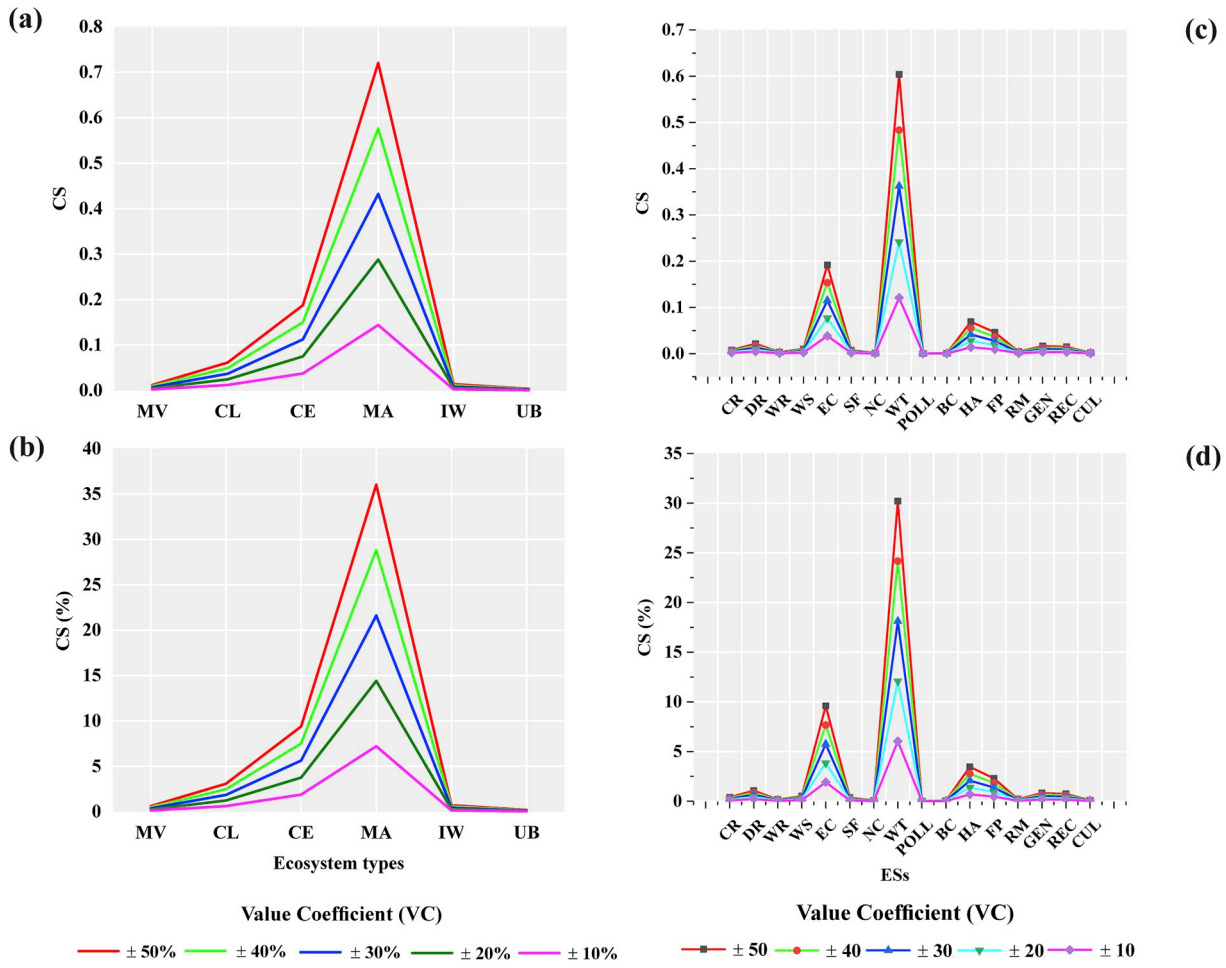

Fig. 9. (a) and (c) shows the coefficient of sensitivity (CS) of ESVs for six ecoregions and 16 ES at five scenarios (± 50%, ± 40%, ± 30%, ± 20%, ± 10%), (b) and (d) shows the percentage of CS at five scenarios.

ESs were measured through spatial trade-offs and synergy analysis (Fig. 13). At the administrative scale, most of the ESs exhibited statistically significant trade-offs and synergies. This suggests that at the administrative level, land degradation and destruction of productive land would incur a substantial loss of the critical ESs, which can't be replenished by any form of human inputs. The WT, EC, DR, HA, and FP services are the main ESs of Sundarbans. Considering the grid level analysis, at 1 km scale, all the 120 pairs are significantly correlated ($p \leq 0.001$) (Table S5). However, the maximum correlation was observed between WT and REC, WT and HA, WT and DR, SFR and GEN, SFR and FP, REC and HA, REC and DR, POL and GEN, HA and DR, and FP and CR services (Table S5). At 5 km scale, amongst the 120 pairs, only five pairs, didn't produce any significant association. For the 10 km spatial grid, six pairs are significant at $p \leq 0.05$, five pairs at $p \leq 0.01$ level, and total 105 pairs at $p \leq 0.001$ level. Additionally, only four pairs are found insignificant at the 10 km grid scale. Considering the 15 km grid scale, total 95 pairs were significantly correlated at $p \leq 0.001$ level, ten pairs at $p \leq 0.01$ level, and five pairs at $P \leq 0.05$ level. Total ten pairs are found insignificant at this scale. At the highest spatial scale (20 km), only 89 pairs are significant at $p \leq 0.001$ level, six pairs at $p \leq 0.01$, and total 13 pairs at $p \leq 0.05$ level. At this scale total, total 108 pairs are found to be significant at different significance levels, whereas, total 12 pairs have produced an insignificant approximation. For the ESs, the trade-offs and synergies values were found insignificant after 3 km, 8 km, 11 km, and 18 km.

In this study, we have observed that despite having less number of samples, the larger scale had produced a higher pairwise association than that of smaller scale, although, in some cases, they are not statistically significant. Xu et al., 2017a,b found that the scale effects on ESs will decrease with spatial scale, as the higher pairwise correlation was observed at a smaller scale and vice versa. This finding is not per our estimates because the significant relationship of any estimate depends on the number of samples, as high pairwise trade-offs and synergies are found insignificant in many cases despite having higher correlation value. Additionally, to carefully asses the land use conflict and its role in producing multiple ESs, it is important to evaluate the pairwise association of the ESs at a spatial level. (Xu et al., 2017a,b).

4.3. Elasticity, sensitivity, and coordination degree - a new approach for environmental impact assessment in natural reserve region

All sensitivity tests including the coefficient of sensitivity, the coefficient of elasticity, ESSI, and coordination degree are collectively indicating the response behavior of the ecosystem to any unprecedented changes. This sensitivity estimates entirely depend on the specificity of the ESVs and the regions under consideration. Additionally, the linear approximation assumed throughout this study may not be reflecting the complex and dynamic behavior of the ecosystem, as we haven't considered the other limiting factors which might have some significant role on controlling the ecosystem response to any unwanted change. Given all sensitivity measures, the mangrove and water bodies including the coastal estuary and inland wetland are found to be highly sensitive to human or natural appropriation. The other ecosystems like cropland, mixed vegetation, and urban land exhibited a moderate to lower sensitivity values for the mentioned changes. Among the specific ESs, the WT, EC, HP, FP, and DR services

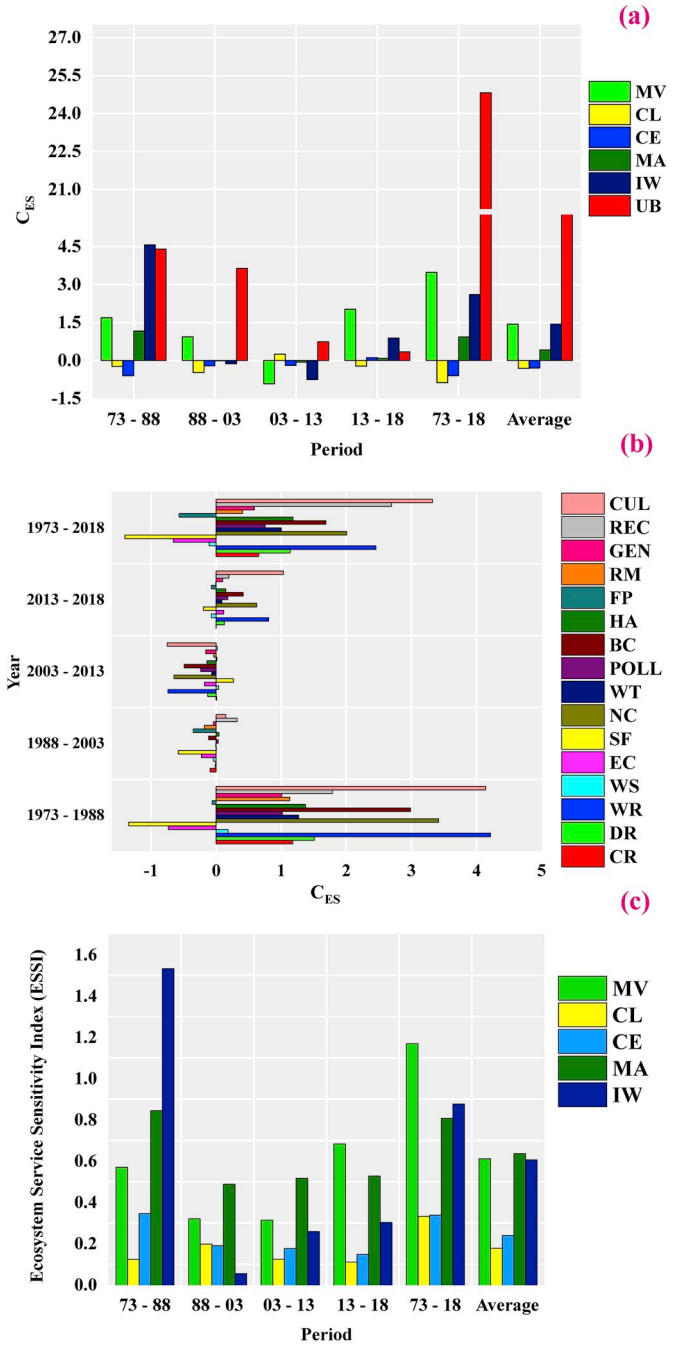

Fig. 10. (a) and (b) shows the coefficient of elasticity (C_{ES}) of the major ecoregions and ESs of Sundarbans for six reference periods, (c) ecosystem service sensitivity index for the major ecoregions of Sundarbans.

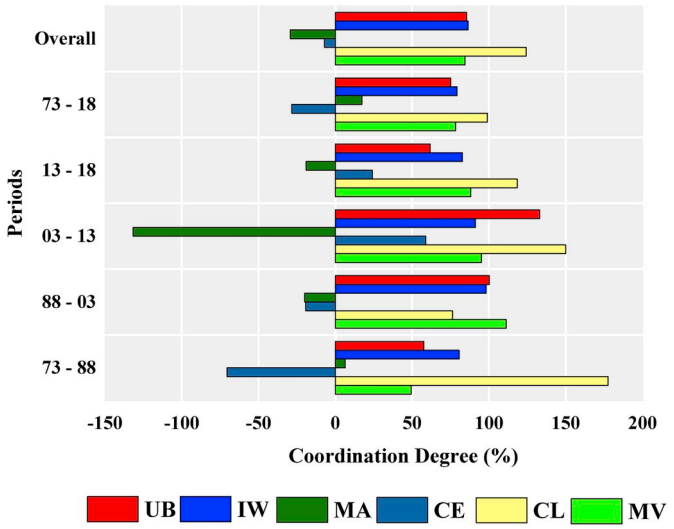

Fig. 11. Shows the coordination degree between the ecosystem service values and land use land cover charges during different reference periods.

were highly sensitive to any natural and human modification.

In this study, we evaluated the response and sensitivity of the major ecosystems of Sundarbans to LULC changes and tried to provide an insight into the possible effects of land conversion on ESs at multiple changing scenarios. Although several protection measures were initiated to preserve the mangrove tract of Sundarbans with the support of forest protection committees (FPC), forest directories (FD), and local stakeholders. Still, the economic values and significance of mangroves in order to produce the essential ESs is somehow unknown or not fully explored. However, it is true that even if these critical services are beneficial for human well-being and subsistence, the valuation estimates of these services has not been directly included in the decision-making process due to the unawareness and methodological uncertainties (Vo et al., 2012). Furthermore, the decision makers and stakeholders involved in the policy-making are not familiar with the quantified values; instead the cost and benefits figures for any environmental impact assessment (EIA). Therefore, accurate estimates of ES valuation and mapping can be a robust tool for assessing the economic and ecological impact of a specific ecosystem and to gauge the effects of faulty decision making and overexploitation of natural resources on ESs. Additionally, the sensitivity measures provided in our study can also be considered in decision making along with the other environmental management measures for better management of natural resources at any given ecosystem and to perform EIA measures more precisely to understand inevitable linkages between the socio-economic development and environmental degradation in a natural reserve region like Sundarbans.

5. Conclusion

In this study, we have calculated the spatiotemporal ESVs of Sundarbans biosphere region (SBR), the largest single mangrove tract in the world. Total 17 ESs were chosen, and their monetary values are estimated using the adjusted equivalent value coefficient. Total five dynamic factors including NPP, precipitation, NDVI, FVC, and yield were used to rectify the global coefficient values. Presently, cropland is the dominant land use type in the study region, and contributes 44.8% to the total geographical extent, followed by coastal estuary (21.95%), mangrove forest (15.9%), mixed vegetation (12.57%), urban built-up (2.38%), inland wetland (2.24%), and sandy coast (0.11%), respectively. On the other side, due to the areal expansion of mangrove cover, the ESVs of CR, DR, WS, NC, WT, HA, RM, GEN, and REC have increased during 1973–2018, whereas, a net decrease of ESVs was observed for EC, SFR, POLL, BC, FP. Whereas, the expansion of inland waterbodies at the expense of cropland and the natural green surface is found significant in this study. This trend occurred in and around the Sandeshkhali, Canning, Minakhan, Haora administrative province due to high rate conversion of shrimp ponds for inland fishing and associated practices. In contrast, we have observed that significant crop areas are lost during this study period. This could be the reason for declining provisioning services in Sundarbans, which is one of the primary sources of livelihoods of the residents of Sundarbans. Given all sensitivity measures, the mangrove and water bodies including the coastal estuary and inland wetland are found to be highly sensitive to any human or natural appropriation. The other ecosystems like cropland, mixed vegetation, and urban land exhibited a moderate to lower

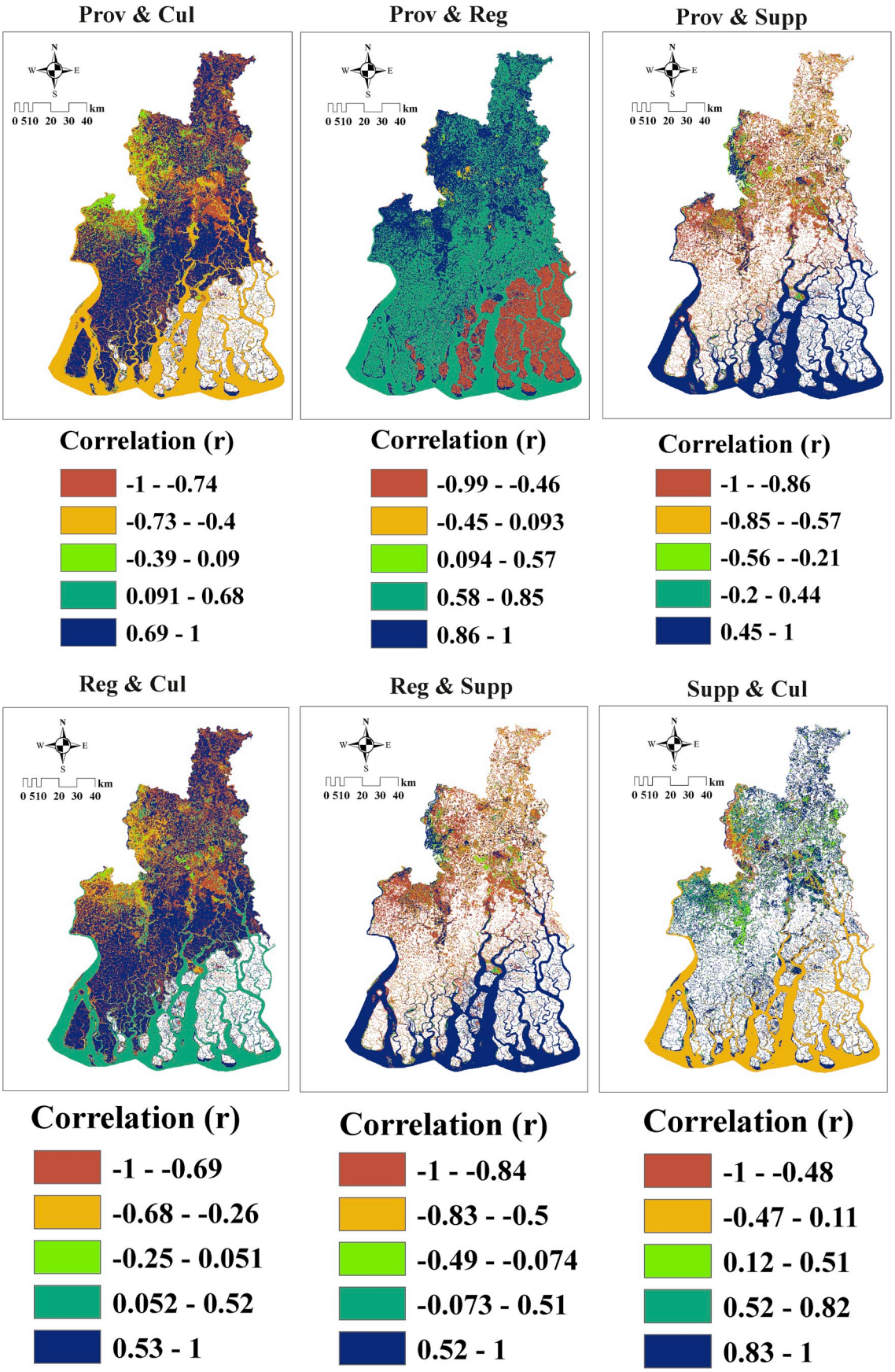

Fig. 12. Spatial association between the four ESs bundles, i.e. Prov = Provisioning, Cul = Cultural, Reg = Regulating, and Supp = Supporting services during the research period.

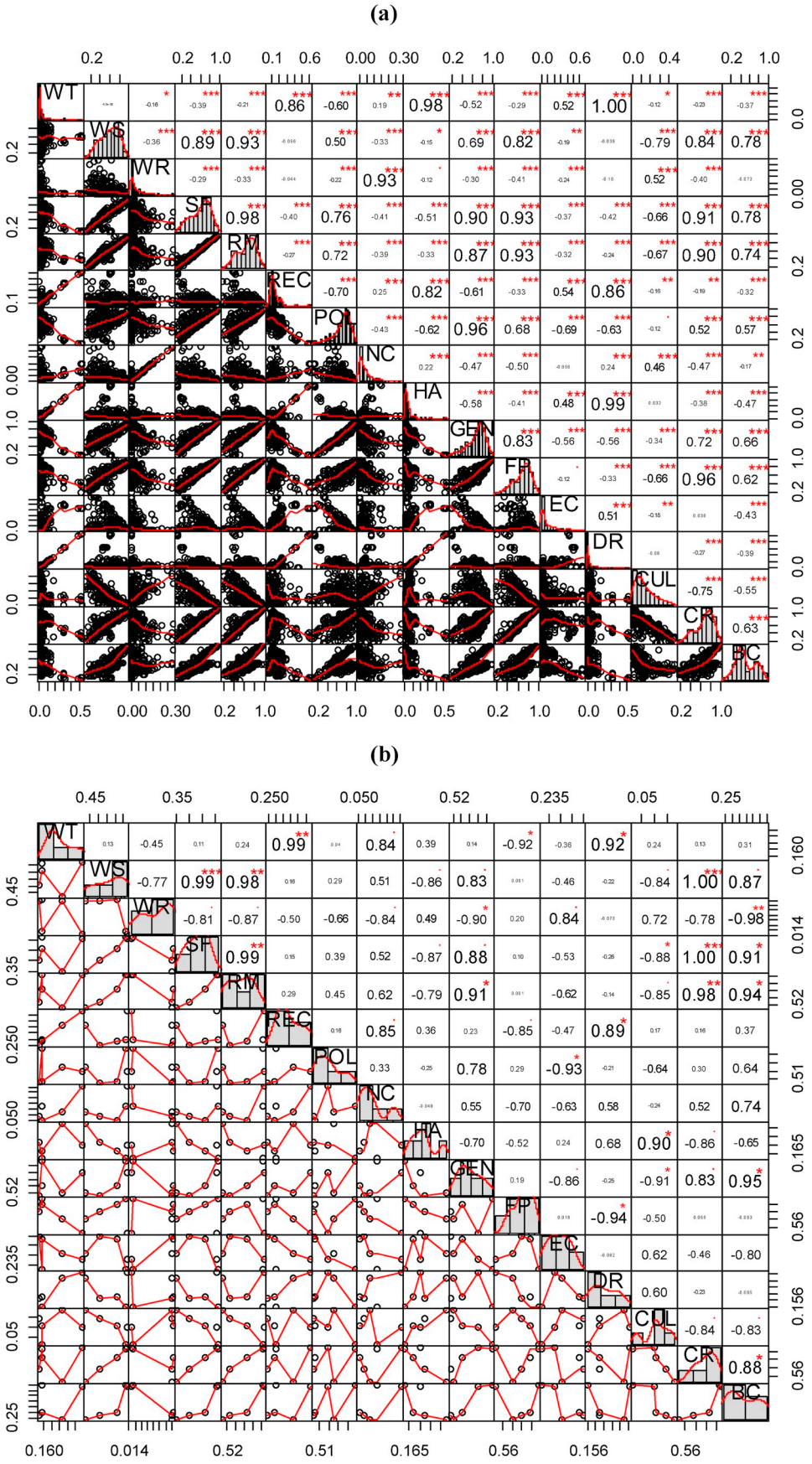

Fig. 13. Scale-dependent synergies and trade-off among the ESs at (a) administrative scale and (b) county scale.

sensitivity values for the mentioned changes. The outcomes of this study could be a helpful document to the land administrators, planner, and environmentalist to understand the inevitable land-resource conflict in the natural reserve region. Additionally, it will provide an important reference to the decision makers to evaluate sensitivity, vulnerability, and resilience of an ecosystem to any unprecedented changes and to formulate suitable biodiversity protection plan for minimizing human pressures on natural goods and services.

Acknowledgment

SS and SC acknowledge the University Grants Commission (UGC) for providing continuous research fellowship for carrying out the research at Indian Institute of Technology (IIT), Kharagpur (India) and Jawaharlal Nehru University, New Delhi. The authors express their sincere gratitude to the anonymous reviewers and the Editorial Board for fruitful and constructive comments to enhance the quality of the paper.

Appendix A. Supplementary data

Supplementary data to this article can be found online at https://doi.org/10.1016/j.jenvman.2019.04.095.

References

Abatzoglou, J.T., Dobrowski, S.Z., Parks, S.A., Hegewisch, K.C., 2018. TerraClimate, a high-resolution global dataset of monthly climate and climatic water balance from 1958–2015. Scientific data 5, 170191.

Akhand, A., Mukhopadhyay, A., Chanda, A., Mukherjee, S., Das, A., Das, S., Hazra, S., Mitra, D., Choudhury, S.B., Rao, K.H., 2017. Potential CO 2 emission due to loss of above ground biomass from the Indian Sundarban mangroves during the last four decades. Journal of the Indian Society of Remote Sensing 45 (1), 147–154.

Boumans, R., Costanza, R., Farley, J., Wilson, M.A., Portela, R., Rotmans, J., Villa, F., Grasso, M., 2002. Modeling the dynamics of the integrated earth system and the value of global ecosystem services using the GUMBO model. Ecol. Econ. 41 (3), 529–560.

Braat, L.C., De Groot, R., 2012. The ecosystem services agenda: bridging the worlds of natural science and economics, conservation and development, and public and private policy. Ecosystem Services 1 (1), 4–15.

Bruel, B.O., Marques, M.C., Britez, R.M., 2010. Survival and growth of tree species under two direct seedling planting systems. Restor. Ecol. 18 (4), 414–417.

Congalton, Russell G., 1991. A review of assessing the accuracy of classifications of remotely sensed data. Rem. Sens. Environ. 37 (1), 35–46.

Costanza, R., d'Arge, R., De Groot, R., Farber, S., Grasso, M., Hannon, B., Limburg, K., Naeem, S., O'neill, R.V., Paruelo, J., Raskin, R.G., 1997. The value of the world's ecosystem services and natural capital. Nature 387 (6630), 253.

Costanza, R., Pérez-Maqueo, O., Martinez, M.L., Sutton, P., Anderson, S.J., Mulder, K., 2008. The value of coastal wetlands for hurricane protection. AMBIO A J. Hum. Environ. 37 (4), 241–248.

Costanza, Robert, Rudolf de, Groot, Paul, Sutton, Sander Van der, Ploeg, Anderson, Sharolyn J., Kubiszewski, Ida, Farber, Stephen, Kerry Turner, R., 2014. Changes in the global value of ecosystem services. Glob. Environ. Change 26, 152–158.

Costanza, R., de Groot, R., Braat, L., Kubiszewski, I., Fioramonti, L., Sutton, P., et al., 2017. Twenty years of ecosystem services: how far have we come and how far do we still need to go? Ecosystem Services 28, 1–16. http://doi.org/10.1016/j.ecoser.2017.09.008.

Curran, L.M., 2004. Lowland forest loss in protected areas of Indonesian Borneo. Science 303 (5660), 1000–1003.

Curtis, I.A., 2004. Valuing ecosystem goods and services: a new approach using a surrogate market and the combination of a multiple criteria analysis and a Delphi panel to assign weights to the attributes. Ecol. Econ. 50 (3–4), 163–194.

Datta, D., Deb, S., 2012. Analysis of coastal land use/land cover changes in the Indian Sunderbans using remotely sensed data. Geo Spat. Inf. Sci. 15 (4), 241–250.

DE Groot, Rudolf S., Matthew Wilson, A., Boumans, Roelof M.J., 2002. A typology for the classification, description and valuation of ecosystem functions, goods and services. Ecol. Econ 41 (3), 393–408.

De Groot, R., Brander, L., Van Der Ploeg, S., Costanza, R., Bernard, F., Braat, L., Christie, M., Crossman, N., Ghermandi, A., Hein, L., Hussain, S., 2012. Global estimates of the value of ecosystems and their services in monetary units. Ecosystem services 1 (1), 50–61.

Dutta, S., Chakraborty, K., Hazra, S., 2017. Ecosystem structure and trophic dynamics of an exploited ecosystem of Bay of Bengal, Sundarban Estuary, India. Fish. Sci. 83 (2), 145–159.

Fei, L., Shuwen, Z., Jiuchun, Y., Liping, C., Haijuan, Y., Kun, B., 2018. Effects of land use change on ecosystem services value in West Jilin since the reform and opening of China. Ecosystem Services 31, 12–20.

Fu, B., Li, Y., Wang, Y., Zhang, B., Yin, S., Zhu, H., Xing, Z., 2016. Evaluation of ecosystem service value of riparian zone using land use data from 1986 to 2012. Ecol. Indicat. 69, 873–881. http://doi.org/10.1016/j.ecolind.2016.05.048.

Giri, C., Pengra, B., Zhu, Z., Singh, A., Tieszen, L.L., 2007. Monitoring mangrove forest dynamics of the Sundarbans in Bangladesh and India using multi-temporal satellite data from 1973 to 2000. Estuar. Coast Shelf Sci. 73 (1–2), 91–100.

Giri, C., Ochieng, E., Tieszen, L.L., Zhu, Z., Singh, A., Loveland, T., Masek, J., Duke, N., 2011. Status and distribution of mangrove forests of the world using earth observation satellite data. Glob. Ecol. Biogeogr. 20 (1), 154–159.

Huang, X., Ma, J.X., 2013. Changes in the ecosystem service values of typical river basins in arid regions of Northwest China. Ecohydrology 6 (6), 1048–1056.

Janalipour, M., Mohammadzadeh, A., 2017. A fuzzy-ga based decision making system for detecting damaged buildings from high-spatial resolution optical images. Rem. Sens. 9 (4), 349.

Keesstra, S., Nunes, J., Novara, A., Finger, D., Avelar, D., Kalantari, Z., Cerdà, A., 2018. The superior effect of nature based solutions in land management for enhancing ecosystem services. Sci. Total Environ. 610, 997–1009.

Khatami, R., Mountrakis, G., Stehman, S.V., 2017. Mapping per-pixel predicted accuracy of classified remote sensing images. Rem. Sens. Environ. 191, 156–167.

Kindu, M., Schneider, T., Teketay, D., Knoke, T., 2016. Science of the Total Environment Changes of ecosystem service values in response to land use/land cover dynamics in Munessa – shashemene landscape of the Ethiopian highlands. Sci. Total Environ. 547, 137–147. http://doi.org/10.1016/j.scitotenv.2015.12.127.

Kreuter, U.P., Harris, H.G., Matlock, M.D., Lacey, R.E., 2001. Change in ecosystem service values in the San Antonio area, Texas. *Ecological economics*. 39 (3), 333–346.

Li, Y., Zhang, H., Xue, X., Jiang, Y., Shen, Q., 2018. Deep learning for remote sensing image classification: a survey. Wiley Interdisciplinary Reviews: Data Min. Knowl. Discov. 8 (6), e1264.

Liu, Y., Li, J., Zhang, H., 2012. An ecosystem service valuation of land use change in Taiyuan City, China. Ecol. Model. 225, 127–132. http://doi.org/10.1016/j.ecolmodel.2011.11.017.

Liu, P., Jiang, S., Zhao, L., Li, Y., Zhang, P., Zhang, L., 2017. What are the benefits of strictly protected nature reserves? Rapid assessment of ecosystem service values in Wanglang Nature Reserve, China. Ecosystem Services 26, 70–78.

Luo, J., Xing, X., Wu, Y., Zhang, W., Chen, R.S., 2018. Spatio-temporal analysis on built-up land expansion and population growth in the Yangtze River Delta Region, China: from a coordination perspective. Appl. Geogr. 96, 98–108.

Liu, Shuang, et al., 2010. Valuing ecosystem services. Ann. N. Y. Acad. Sci. 1185 (1), 54–78.

Mandal, S.K., Dey, M., Ganguly, D., Sen, S., Jana, T.K., 2009. Biogeochemical controls of arsenic occurrence and mobility in the Indian Sundarban mangrove ecosystem. Mar. Pollut. Bull. 58 (5), 652–657.

Mandal, S., Debnath, M., Ray, S., Ghosh, P.B., Roy, M., Ray, S., 2012. Dynamic modelling of dissolved oxygen in the creeks of Sagar island, Hooghly–Matla estuarine system, West Bengal, India. Appl. Math. Model. 36 (12), 5952–5963.

Mandal, S.K., Ray, R., Chowdhury, C., Majumder, N., Jana, T.K., 2013. Implication of organic matter on arsenic and antimony sequestration in sediment: evidence from Sundarban mangrove forest, India. Bull. Environ. Contam. Toxicol. 90 (4), 451–455.

Maxwell, A.E., Warner, T.A., Fang, F., 2018. Implementation of machine-learning classification in remote sensing: an applied review. Int. J. Remote Sens. 39 (9), 2784–2817.

MEA (Millennium Ecosystem Assessment), 2005. Ecosystems and Human Well-Being: Synthesis. pp. 155.

Nandy, S., Kushwaha, S.P.S., 2010. Geospatial modelling of biological richness in Sunderbans. Journal of the Indian Society of Remote Sensing 38 (3), 431–440.

Nandy, S., Kushwaha, S.P.S., 2011. Study on the utility of IRS 1D LISS-III data and the classification techniques for mapping of Sunderban mangroves. J. Coast. Conserv. 15 (1), 123–137.

Nelson, E., Mendoza, G., Regetz, J., Polasky, S., Tallis, H., Cameron, D., Chan, K.M., Daily, G.C., Goldstein, J., Kareiva, P.M., Lonsdorf, E., 2009. Modeling multiple ecosystem services, biodiversity conservation, commodity production, and tradeoffs at landscape scales. Front. Ecol. Environ. 7 (1), 4–11.

Olofsson, P., Foody, G.M., Stehman, S.V., Woodcock, C.E., 2013. Making better use of accuracy data in land change studies: estimating accuracy and area and quantifying uncertainty using stratified estimation. Remote Sens. Environ. 129, 122–131.

Olofsson, P., Foody, G.M., Herold, M., Stehman, S.V., Woodcock, C.E., Wulder, M.A., 2014. Good practices for estimating area and assessing accuracy of land change. Remote Sens. Environ. 148, 42–57.

Pontius Jr., R.G., Millones, M., 2011. Death to Kappa: birth of quantity disagreement and allocation disagreement for accuracy assessment. Int. J. Remote Sens. 32 (15), 4407–4429.

Rakshit, D., Sarkar, S.K., Bhattacharya, B.D., Jonathan, M.P., Biswas, J.K., Mondal, P., Mitra, S., 2015. Human-induced ecological changes in western part of Indian Sundarban megadelta: a threat to ecosystem stability. Mar. Pollut. Bull. 99 (1–2), 186–194.

Ren, Y., Lü, Y., Fu, B., 2016. Quantifying the impacts of grassland restoration on biodiversity and ecosystem services in China: a meta-analysis. Ecol. Eng. 95, 542–550. http://doi.org/10.1016/j.ecoleng.2016.06.082.

Sannigrahi, S., Rahmat, S., Chakraborti, S., Bhatt, S., Jha, S., 2017. Changing dynamics of urban biophysical composition and its impact on urban heat island intensity and thermal characteristics: the case of Hyderabad City, India. Modeling Earth Systems and Environment 3 (2), 647–667.

Sannigrahi, S., Bhatt, S., Rahmat, S., Paul, S.K., Sen, S., 2018a. Estimating global ecosystem service values and its response to land surface dynamics during 1995–2015. J. Environ. Manag. 223, 115–131.

Sannigrahi, S., Bhatt, S., Rahmat, S., Uniyal, B., Banerjee, S., Chakraborti, S., Jha, S., Santra, K., Bhatt, A., 2018b. Analyzing the role of biophysical compositions in

minimizing urban land surface temperature and urban heating. Urban climate 24, 803–819.
Song, W., Deng, X., 2017. Land-use/land-cover change and ecosystem service provision in China. Sci. Total Environ. 576, 705–719. http://doi.org/10.1016/j.scitotenv.2016.07.078.
Song, Wei, et al., 2015. Impacts of land-use change on valued ecosystem service in rapidly urbanized North China Plain. Ecol. Model. 318, 245–253.
Stehman, S.V., Wickham, J.D., 2011. Pixels, blocks of pixels, and polygons: choosing a spatial unit for thematic accuracy assessment. Remote Sens. Environ. 115 (12), 3044–3055.
TEEB, 2010. In: Kumar, Pushpam (Ed.), The Economics of Ecosystems and Biodiversity: Ecological and Economic Foundations. Earthscan, London and Washington.
Tolessa, T., Senbeta, F., Kidane, M., 2017. The impact of land use/land cover change on ecosystem services in the central highlands of crossmark. Ecosystem Services 23 (December 2016), 47–54. http://doi.org/10.1016/j.ecoser.2016.11.010.
Troy, A., Wilson, M.A., 2006. Mapping ecosystem services: practical challenges and opportunities in linking GIS and value transfer. Ecol. Econ. 60 (2), 435–449.
Viña, A., Liu, J., 2017. Hidden roles of protected areas in the conservation of biodiversity and ecosystem services. Ecosphere 8 (6).
Vo, Q.T., Kuenzer, C., Vo, Q.M., Moder, F., Oppelt, N., 2012. Review of valuation methods for mangrove ecosystem services. Ecol. Indicat. 23, 431–446.
Wagner, J.E., Stehman, S.V., 2015. Optimizing sample size allocation to strata for estimating area and map accuracy. Remote Sens. Environ. 168, 126–133.
Wang, Y., Gao, J., Wang, J., Qiu, J., 2014. Value assessment of ecosystem services in nature reserves in Ningxia, China: a response to ecological restoration. PLoS One 9 (2).
Wang, Z., Wang, Z., Zhang, B., Lu, C., Ren, C., 2015. Impact of land use/land cover changes on ecosystem services in the Nenjiang River Basin, Northeast China. Ecological Processes 4 (1) 11.e89174.
Wilson, M.A., Hoehn, J.P., 2006. Valuing Environmental Goods and Services Using Benefit Transfer: the State-Of-The Art and Science.
Xie, G.D., Lu, C.X., Leng, Y.F., Zheng, D., Li, S.C., 2003. Ecological assets valuation of the Tibetan Plateau. J. Nat. Resour. 18 (2), 189–196.
Xie, G.D., Zhen, L., Lu, C.X., Xiao, Y., Chen, C., 2008. Expert knowledge based valuation method of ecosystem services in China. J. Nat. Resour. 23 (5), 911–919.
Xie, G., Zhang, C., Zhen, L., Zhang, L., 2017. Dynamic changes in the value of China's ecosystem services. Ecosystem Services 26, 146–154.
Xu, W., Xiao, Y., Zhang, J., Yang, W., Zhang, L., Hull, V., Wang, Z., Zheng, H., Liu, J., Polasky, S., Jiang, L., 2017a. Strengthening protected areas for biodiversity and ecosystem services in China. Proc. Natl. Acad. Sci. Unit. States Am. 114 (7), 1601–1606.
Xu, S., Liu, Y., Wang, X., Zhang, G., 2017b. Scale effect on spatial patterns of ecosystem services and associations among them in semi-arid area: a case study in Ningxia Hui Autonomous Region, China. Sci. Total Environ. 598, 297–306.
Yang, Y., Xiao, P., Feng, X., Li, H., 2017. Accuracy assessment of seven global land cover datasets over China. ISPRS J. Photogrammetry Remote Sens. 125, 156–173.
Yi, H., Güneralp, B., Filippi, A.M., Kreuter, U.P., Güneralp, İ., 2017. Impacts of Land Change on Ecosystem Services in the San Antonio River Basin , Texas , from 1984 to 2010, vol. 135. pp. 125–135. http://doi.org/10.1016/j.ecolecon.2016.11.019.
Yoshida, A., Chanhda, H., Ye, Y.M., Liang, Y.R., 2010. Ecosystem service values and land use change in the opium poppy cultivation region in Northern Part of Lao PDR. Acta Ecol. Sin. 30 (2), 56–61. http://doi.org/10.1016/j.chnaes.2010.03.002.
Yu, Dandan, Han, Shijie, 2016. Ecosystem service status and changes of degraded natural reserves–A study from the Changbai Mountain Natural Reserve, China. Ecosyst. Serv. 20, 56–65.
Yushanjiang, A., Zhang, F., Yu, H., Kung, H., 2018. Quantifying the spatial correlations between landscape pattern and ecosystem service value: a case study in Ebinur Lake Basin, Xinjiang, China. Ecol. Eng. 113, 94–104. March 2017. http://doi.org/https://doi.org/10.1016/j.ecoleng.2018.02.005.
Zhang, B., Shi, Y.T., Liu, J.H., Xu, J., 2017. Economic values and dominant providers of key ecosystem services of wetlands in Beijing, China. Ecol. Indicat. 77, 48–58.
Zhu, X.X., Tuia, D., Mou, L., Xia, G.S., Zhang, L., Xu, F., Fraundorfer, F., 2017. Deep learning in remote sensing: a comprehensive review and list of resources. IEEE Geoscience and Remote Sensing Magazine 5 (4), 8–36.